CHAPTER 6

# Hydrogen Interactions with Polycrystalline and Amorphous Silicon—Theory

*Chris G. Van de Walle*

XEROX PALO ALTO RESEARCH CENTER
PALO ALTO, CALIFORNIA



## I. Introduction

### 1. ROLE OF HYDROGEN IN AMORPHOUS AND POLYCRYSTALLINE SILICON

Hydrogen is known to interact with silicon in a wide variety of ways, including passivation of the surface, passivation of shallow as well as deep levels, generation of extended defects, etc. (Pankove and Johnson, 1991; Pearton *et al.*, 1992). In amorphous and polycrystalline silicon, hydrogen passivates dangling bonds and eliminates deep levels from the bandgap,




ISBN 0-12-752170-4

thereby dramatically improving the electronic quality of the material (Street, 1991a). However, hydrogen also has been established to play a role in creating metastable defects. Over the years, many models have been proposed to describe hydrogen diffusion and the creation and annihilation of defects. To put these models on a firmer basis, however, quantitative information is required on the energetics of the various processes and reactions. Such information is very hard to obtain directly from experiment, but it can be generated using computational techniques.

In this chapter I will focus on a review of theoretical approaches that include some computational component. I do not plan to give an exhaustive overview of the various computational approaches that have been used to generate amorphous networks; this could be the topic of a review chapter in its own right. I will refer to results from these approaches only when they address issues that are of direct relevance to the understanding of the interaction of hydrogen with the network.

In Section I.2 I will review some of the general features of hydrogen interactions with silicon. Many of these features actually apply to H interactions with semiconductors in general, but here the focus is on silicon. Most of the basic properties were first derived for hydrogen in a crystalline environment (see the reviews by Van de Walle, 1991a, 1991b; Estreicher, 1995), but the results also have bearing on amorphous materials.

The various computational techniques that have been used in the study of hydrogen interactions with polycrystalline or amorphous silicon (*a*-Si) will be discussed briefly in Section I.3.

## 2. General Features of Hydrogen in Silicon

### *a. Isolated Interstitial Hydrogen*

Isolated interstitial hydrogen can assume different charge states in silicon. The impurity introduces a level in the bandgap, and the charge state depends on the occupation of that level. The charge state determines the most favorable location of hydrogen in the semiconductor lattice.

$H^+$ In the positive charge state (essentially a proton), hydrogen seeks out regions of high electronic charge density. In silicon, the maximum charge density is found at the bond-center (BC) site. The stability of the BC configuration arises from the formation of a three-center bond between the H atom and the two Si neighbors (Van de Walle, 1991b). $H^+$ is the preferred charge state in *p*-type material.

$H^-$ In the negative charge state, hydrogen prefers regions of low electronic charge density, i.e., at the tetrahedral interstitial site. $H^-$ is the preferred charge state in *n*-type material.

$H^0$ The lattice location of neutral hydrogen ($H^0$) is quite sensitive to the details of the charge density distribution. In crystalline Si, $H^0$ is located at BC; however, the energy of $H^0$ is always higher than that of $H^+$ or $H^-$; i.e., the neutral charge state is never the most stable state. This is the defining characteristic of a negative-*U* center.

The charge states of interstitial H in *a*-Si have not been established conclusively, but it is plausible that they would follow the same trends as for H in crystalline Si (*c*-Si).

Since H at the BC site is such an important configuration, it is useful to look in more detail at the basic atomic and electronic structure. Three-center bonds (Si—H—Si) were actually suggested for H in *a*-Si:H as early as 1978 by Fisch and Licciardello (1978). These bonds were studied in more detail by Zacher *et al.* (1986). As mentioned earlier, the stability arises because of Coulomb attraction between the proton and the high electron density at the bond center. At the same time, however, the stability is reduced due to the geometric constraints imposed by the surrounding network; in order to provide reasonable Si—H bonding distances, the Si atoms have to move outward from their regular lattice sites in *c*-Si, raising the elastic energy. Insertion of H into a bond that has a longer bond length than the equilibrium Si—Si bond length therefore increases the stability; this issue will be discussed in Sections II.4 and III.3.

### *b. Diffusion*

Hydrogen, being a small and light impurity, is expected to move quite easily through the perfect lattice. The calculated migration barrier for the positive and neutral charge states in *c*-Si is 0.2 eV; for the negative charge state it is 0.25 eV (Van de Walle *et al.*, 1989). Interstitial hydrogen in *a*-Si:H is expected to move with similar ease. However, in *a*-Si:H there is the possibility for hydrogen to become trapped at traps with various energy depths; a schematic of a possible diffusion process is shown in Fig. 1. The diffusion process therefore becomes quite complicated, with a measured activation energy of around 1.5 eV. A rigorous microscopic explanation for this phenomenon is not yet in place; various models will be discussed in Section III, along with attempts to associate specific energy values with the levels depicted in Fig. 1.

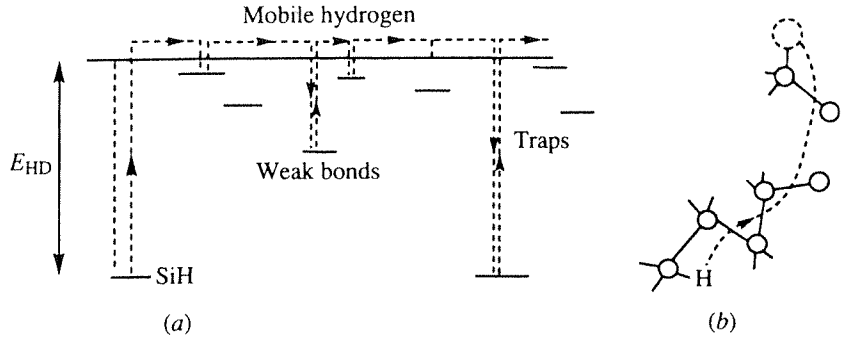


FIG. 1. Schematic diagram of the possible hydrogen diffusion mechanisms: (a) the potential wells corresponding to the trapping sites and the energy of the mobile hydrogen; (b) the motion of the hydrogen through the network. (From Street, 1991a.)

### c. *Compensation and Passivation of Shallow Impurities*

Based on the characteristics of isolated interstitial hydrogen, one can immediately predict that hydrogen will interact with shallow dopants. Hydrogen always counteracts the electrical activity of the dopants. The presence of hydrogen in *p*-type material leads to formation of $H^+$, a donor, which compensates acceptors. $H^+$ can form a complex with the acceptor impurity, to which it is coulombically attracted. Similarly, $H^-$ passivates donors.

### d. *Interactions with Deep Levels*

Hydrogen, of course, also can interact with impurities or defects that form deep levels in the bandgap. A prime example is the interaction of hydrogen with dangling bonds in amorphous silicon, a process that significantly improves the electronic quality of the material. One expects hydrogen to interact with extended defects as well.

### e. *Hydrogen Molecules and Molecular Complexes*

Theory predicts that $H_2$ molecules readily form in silicon; the binding energy is somewhat smaller than its value in free space but still large enough to make interstitial $H_2$ one of the more favorable configurations hydrogen can assume in the lattice. Another configuration involving two hydrogen atoms is the so-called $H_2^*$ complex, in which a host-atom bond is broken

and one hydrogen atom is inserted between the two atoms, in a BC position, while the other hydrogen occupies an antibonding (AB) site (Chang and Chadi, 1989). This configuration is somewhat higher in energy than the $H_2$ molecule, but it may play an important role in diffusion, in metastability, as well as in nucleation of larger hydrogen-induced defects.

### *f. Extended Hydrogen Complexes*

It has been observed that hydrogenation can induce microdefects in a region within $\sim 1000$ Å of the surface (Johnson *et al.*, 1987, 1991; Ponce *et al.*, 1987). The defects, studied with transmission electron microscopy (TEM), have the appearance of platelets along $\{111\}$ crystallographic planes and range in size from 50 up to 1000 Å. One or two H atoms per Si—Si bond are present. Several models have been proposed for the structure of these platelets (Ponce *et al.*, 1987; Van de Walle *et al.*, 1989; Zhang and Jackson, 1991); the model of Zhang and Jackson (1991) has been worked out in greatest detail. It consists of double-layer $\{111\}$ H platelets resulting from clustering of diatomic $H_2^*$ complexes; this clustering occurs because a certain amount of binding energy can be gained when bringing $H_2^*$ complexes together. However, a definitive experimental microscopic identification of the platelet structure is still lacking. Zhang and Jackson (1991) suggested that similar structures exist in *a*-Si:H. Nickel *et al.* (1996) have observed hydrogen-induced platelets in polycrystalline Si.

### *g. Energies of Various Configurations of H in Si*

First-principles calculations for a large number of configurations of H in Si were discussed by Van de Walle (1994). The results are summarized in Fig. 2. The calculated values were all obtained within a consistent theoretical framework (pseudopotential-density-functional theory) and provide direct information about the relative stability of different configurations.

## 3. COMPUTATIONAL APPROACHES

### *a. Pseudopotential-Density-Functional Calculations*

This computational approach is now regarded as a standard for performing first-principles studies of defects or impurities in semiconductors. Density-functional theory (DFT) in the local density approximation (LDA) (Hohenberg and Kohn, 1964; Kohn and Sham, 1965) allows a description

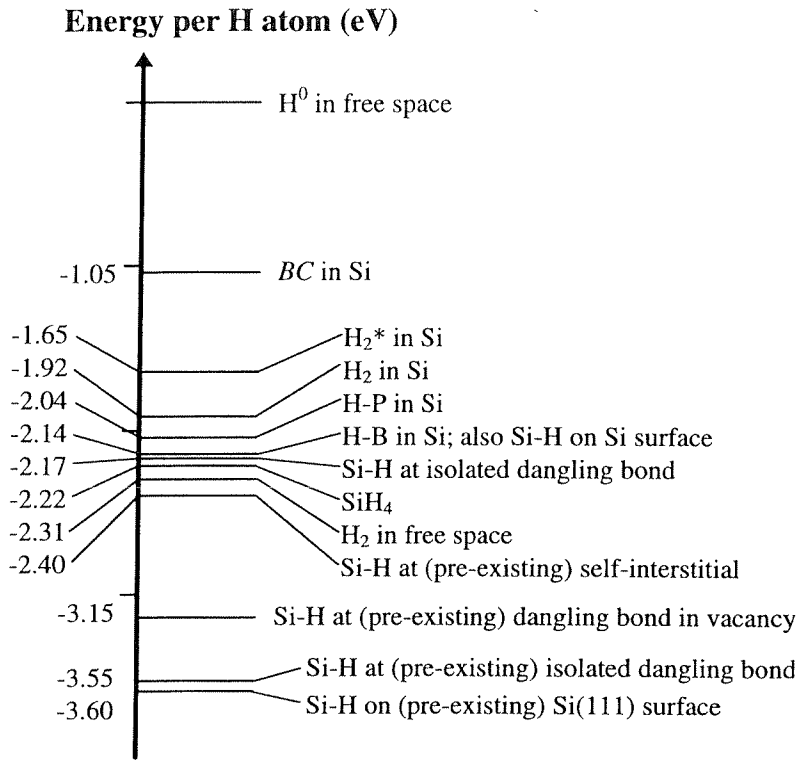


FIG. 2. First-principles energies for various configurations of H in Si. The zero of energy corresponds to a free H atom. The energy values were determined with first-principles pseudopotential-density-functional calculations and include zero-point energies.

of the ground state of the many-body system in terms of a one-electron equation with an effective potential. The total potential consists of an ionic potential due to the atomic cores, a Hartree potential, and a so-called exchange and correlation potential that describes the many-body aspects. This approach has proven very successful for a wide variety of solid-state problems. One shortcoming of the technique is its failure to produce reliable excited-state properties, widely referred to as the "bandgap problem." Many useful results of the calculations depend on ground-state properties and thus are not affected by this shortcoming. In cases where the bandgap enters the calculations either directly or indirectly, judicious inspection of the results may still allow extraction of reliable information.

Most properties of molecules and solids are determined by the valence electrons; the core electrons usually can be removed from the problem by

representing the ionic core (i.e., nucleus plus inner shells of electrons) with a pseudopotential. State-of-the-art calculations employ nonlocal norm-conserving pseudopotentials (Hamann *et al.*, 1979) that are generated solely based on atomic calculations and do not include any fitting to experiment.

The last ingredient commonly used in pseudopotential-density-functional calculations for defects or impurities is the supercell geometry. Ideally, one would like to describe a single isolated impurity in an infinite crystal. In the supercell approach, the impurity is surrounded by a finite number of semiconductor atoms, and this structure is periodically repeated. Maintaining periodicity allows continued use of algorithms such as Fast Fourier Transforms. One also can be assured that the band structure of the host crystal is well described (which may not be the case in a cluster approach). For sufficiently large supercells, the properties of a single, isolated impurity can be derived. Convergence tests have indicated that the energetics of impurities and defects are usually well described by using 32-atom supercells. The supercell approach also allows simulations of nonperiodic systems such as amorphous networks. Periodic boundary conditions still apply to the overall supercell, but within that cell an amorphous system consisting of tens or even hundreds of atoms can be simulated.

An alternative to the use of supercells for systems lacking periodicity is to employ a cluster geometry; a cluster of finite size is usually terminated with H atoms. This approach also can be used to model a defect or impurity in the solid. Whether using supercells (periodic boundary conditions) or clusters, convergence of the results with respect to cell size or cluster size always should be carefully checked.

Finally, I mention that the pseudopotential-density-functional method can be combined with a molecular dynamics approach, as pioneered by Car and Parrinello (1985). In molecular dynamics, atoms in the system move according to calculated forces; simulations can be performed as a function of temperature, mimicking, for instance, quenching of a system from the melt. The computational effort involved in first-principles molecular dynamics usually limits the size of the system, as well as the number of timesteps during which the evolution of the system can be studied.

### *b. Approximate Pseudopotential-Density-Functional Calculations Using the Harris Functional*

To overcome the computational demands of the pseudopotential-density-functional method, Sankey and Niklewski (1989) and Sankey and Drabold (1991) developed an approximate method based on the Harris-functional approach (Harris, 1985) that eliminates the iterative approach typical for

self-consistent calculations. Other approximations used by these authors include a limited basis set consisting of four local orbitals per site. The approach has been used by Fedders and Drabold (1993), Fedders (1995), and Tuttle and Adams (1996) to study amorphous systems containing up to several hundred atoms.

### c. *Empirical Potentials*

As mentioned earlier, the computational complexity of first-principles calculations severely limits the size of systems that can be studied or the length of time over which molecular dynamics simulations can be performed. Various attempts have been made to describe the system of Si and H atoms with empirical potentials. For Si, such potentials have achieved a reasonable degree of reliability; modeling the Si-H interaction, however, has proved very difficult. Indeed, capturing the very different behavior of H in a covalent Si—H bond and in a three-center BC configuration is a challenge. One attempt was made by Biswas *et al.* (1991). Later, the same group went on to develop a tight-binding approach.

### d. *Tight-Binding Molecular Dynamics*

Li and Biswas (1994a, 1995a, 1995b) have devised a tight-binding molecular dynamics approach that can be applied to systems containing several hundred atoms. First-principles calculations would not be feasible for systems of this size. The electronic states are approximated by a superposition of atomic orbitals. Parameters are obtained by fitting to first-principles calculations as well as to experimental values. Li and Biswas (1994a, 1994b) were able to successfully model a wide range of properties of crystalline Si, Si—H vibrational properties, and the total-energy surface for H in *c*-Si. They also found a good description of the electronic and structural properties of *a*-Si:H.

## II. Hydrogen Interactions with Amorphous Silicon

### 1. HYDROGEN MOTION—INTRODUCTION

Hydrogen passivation of dangling-bond defects leads to a significant improvement in the electronic properties of amorphous Si (*a*-Si). The behavior of hydrogen in the amorphous material, however, is complex and

still not fully understood. Hydrogen diffusion through the material is known to be affected by the doping level; in undoped samples, the activation energy $E_A$ is 1.4–1.5 eV; in doped samples, the activation energy is smaller, 1.2–1.3 eV (Street *et al.*, 1987). Hydrogen diffusion is also known to be affected by the presence of free carriers (Santos *et al.*, 1991). In addition, hydrogen motion has been shown to be correlated with the *formation* of both metastable and equilibrium defects (Jackson and Kakalios, 1989).

A central process in these phenomena is the breaking of a silicon-hydrogen bond, in which hydrogen is promoted from a stable configuration (in which it is strongly bonded to a Si atom) to a higher-energy interstitial position (in which it is mobile and can easily move through the lattice). This basic framework was established by Street *et al.* (1987) and is illustrated in Fig. 3. The following reaction describes the breaking of a Si—H

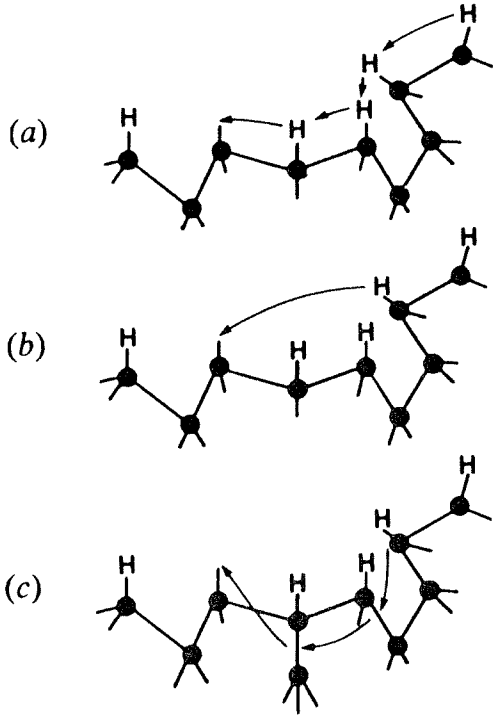


FIG. 3. Schematic diagrams showing three diffusion models for hydrogen in *a*-Si:H: (a) hydrogen moving to an immediately adjacent dangling bond; (b) hydrogen released into an interstitial site and diffusing until it is trapped by a dangling bond; (c) hydrogen released into an interstitial site and then breaking a weak Si—Si bond. (From Street *et al.*, 1987.)

bond and insertion of H into a Si—Si bond, leaving a dangling bond (db) behind:

$$\text{Si—H} + \text{Si—Si} \leftrightarrow \text{Si—H—Si} + \text{db} \tag{1}$$

This reaction has been invoked in the context of defect creation; this picture, based on bond breaking and weak-bond to dangling-bond conversion, is commonly accepted now (Stutzmann *et al.*, 1985; Smith and Wagner, 1987; Street and Winer, 1989; Street, 1991a). The process described by Eq. (1) has been suggested as the microscopic model for light-induced degradation (the Staebler-Wronski effect; Staebler and Wronski, 1977).

Equation (1) also has been used commonly to describe hydrogen diffusion, which proceeds by hydrogen being released from deep or shallow traps and moving in a transport state. A critical discussion of the use of Eq. (1) to describe diffusion can be found in Tuttle and Adams (1998).

Pantelides (1987a) suggested that diffusion and defect annihilation in *a*-Si:H could not be explained solely by invoking motion of hydrogen; he proposed that migration of the intrinsic defects themselves (in particular, floating bonds; Pantelides, 1986) played an important role. Pantelides (1987b) also proposed an explanation for the Staebler-Wronski effect based on floating bonds. Few additional investigations of this hypothesis have been performed; arguments against this proposal were discussed by Street (1991a).

Several groups contributed to the description of H diffusion through *a*-Si (Carlson and Magee, 1978; Street, 1991b, 1991c; Santos and Jackson, 1992; Kemp and Branz, 1993). The key energies that play a role in the diffusion process are illustrated in Fig. 4a. The quantity $E_{\text{Si-H}}$ represents the energy of a Si—H bond. $\mu_{\text{H}}$ is the chemical potential of H atoms. $E_{\text{BC}}$ is the energy of an isolated interstitial H atom at its most stable site in the network; by analogy with crystalline Si (*c*-Si), this is taken to be at the bond-center (BC) site. $E_{\text{S}}$, finally, is the energy corresponding to the saddle point of migration of an interstitial H atom. Figure 4b illustrates the expected broadening of the energy levels in hydrogenated amorphous Si (*a*-Si:H) due to the atomic disorder (Street, 1991b, 1991c).

The hydrogen chemical potential $\mu_{\text{H}}$ determines the occupancy of various configurations; states with energies below $\mu_{\text{H}}$ are (mostly) occupied with hydrogen, and those above are (mostly) empty. The energy difference between mobile hydrogen (energy $E_{\text{S}}$) and $\mu_{\text{H}}$ determines the number of hydrogen atoms that can participate in diffusion. The diffusion activation energy $E_{\text{A}}$ (1.4–1.5 eV in undoped material) therefore should be associated with $E_{\text{S}} - \mu_{\text{H}}$ (Street, 1991b).

Estimates about other energies in Fig. 4 also can be made. Hydrogen diffusion experiments in *c*-Si (Van Wieringen and Warmoltz, 1956) as well

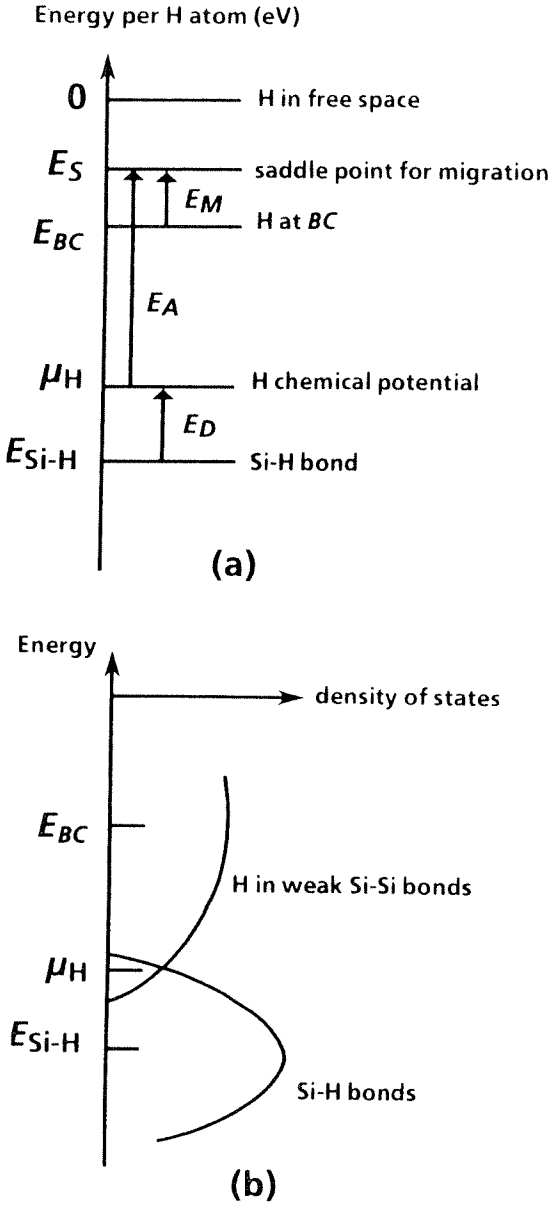


FIG. 4. (a) Energies relevant for H interactions with silicon. The various quantities are described in the text. (b) Schematic hydrogen density of states distribution in *a*-Si, corresponding to the level scheme in (a). The broadening of the levels is due to the disorder in the amorphous network. (From Van de Walle and Street, 1995.)

as H diffusion in *a*-Si when all deep traps are saturated (Santos and Jackson, 1992) indicate that the migration energy $E_M = E_S - E_{BC}$ is about 0.5 eV. On the other hand, first-principles calculations of the adiabatic energy surface (Van de Walle *et al.*, 1989) indicate that $E_M$ is only about 0.2 eV. I will therefore assume a range of values, 0.2–0.5 eV, for $E_M$. Analysis of solubility data in *c*-Si places $E_{BC}$ at about 1 eV below the energy of a H atom in free space (Herring and Johnson, 1991), a value that agrees well with the theoretical value in Fig. 2 (Van de Walle, 1994). Finally, the energy difference between $E_{Si-H}$ and $\mu_H$ can be associated with the dangling-bond formation energy, since the removal of H from Si—H results in a dangling bond; measurement of equilibrium-defect densities indicated that $E_D = \mu_H - E_{Si-H}$ is about 0.2–0.5 eV (Street and Winer, 1989; Street, 1991b).

Inspection of these values leads to a seemingly puzzling result: Based on the numbers quoted earlier, the energy difference between $E_{BC}$ and $E_{Si-H}$ should be around 1.5 eV or less; hence the energy $E_{Si-H}$ would be less than 2.5 eV below the energy of a free H atom. This energy is much smaller (by more than 1 eV) than one would expect based on estimates of binding energies of Si—H bonds, e.g., in a silane ($SiH_4$) molecule. Indeed, it takes 3.92 eV to remove the first H atom from an $SiH_4$ molecule (i.e., $SiH_3$—H) (Walsh, 1981).

One explanation that was proposed assumes that H would be bonded predominantly in strong Si—H bonds on void surfaces and that transport would take place along these internal surfaces (Jackson and Tsai, 1992). The transport level would then be $\sim$1.5 eV about the Si—H energy, meaning that it would lie significantly lower than in *c*-Si (as implied in Fig. 4). There are several problems with this picture. First, there is no evidence that the void structure in *a*-Si could allow for long-range diffusion in this fashion; this has been highlighted in the first-principles calculations for *a*-Si:H structures by Tuttle and Adams (1998). The theoretical results of Van de Walle and Street (1995) also do not support this mechanism.

In order to examine the validity of the framework described by Fig. 4, and to address the apparent inconsistent energetics, values for the various energies included in Fig. 4 can be calculated. In the following sections I will address the energetics of various configurations that hydrogen can assume in *a*-Si. In Section II.2 I focus on H interacting with dangling bonds, first in a crystalline environment and then in an amorphous network. In Section II.3 I discuss the interaction of H with overcoordination defects. Section II.4 describes calculations addressing the energetics of hydrogen insertion in weak Si—Si bonds. In Section II.5 I discuss simulations for amorphous networks that provide information about energy distributions for the various configurations. In Section II.6 I will return to the discussion of hydrogen diffusion and defect formation.

## 2. HYDROGEN INTERACTIONS WITH DANGLING BONDS

Until recently, little information has been available about the energetics of the Si—H bond in bulk (crystalline or amorphous) Si. It had been assumed that the bond strength would be similar to that in a silane ($SiH_4$) molecule, but then effects of the crystalline environment and possible distortions of the bonding configurations are ignored. As a first step, a study was performed for Si—H bonds in a crystalline environment (Van de Walle and Street, 1994). Even though that study did not explicitly take the amorphous nature of the network into account, it was argued that major features of the interaction would be mostly sensitive to the local environment, which is very similar in the crystalline and amorphous cases. Certain types of information, such as repulsion between neighboring H atoms and dissociation mechanisms of the Si—H bond, are also expected to be general in nature. These results are discussed in Section II.2.a. More recently, explicit calculations have been performed for H in an amorphous environment. These results are discussed in Section II.2.b.

### *a. Si—H Bonds Calculated in a Crystalline Environment*

One way to define an energy for the Si—H bond is to address the question, How much energy is needed to remove the H atom from a Si—H bond, leaving a dangling bond behind and placing the hydrogen in an interstitial (BC) position? The resulting energy is a *binding energy*. Pseudopotential-density-functional theory (see Sec. I.3.a) was used to investigate the structure and energy of the Si—H bond in a number of distinct configurations (Van de Walle and Street, 1994). The first geometry was that of the hydrogenated vacancy; here the H atoms are close enough to significantly interact. The binding energy to remove one hydrogen from a fully hydrogenated vacancy was found to be 2.10 eV.

A second geometry placed a dangling bond in a larger void, created by the removal of four Si atoms. For the latter configuration it was found that the energy required to move the H atom from the Si—H bond to an interstitial position is 2.5 eV. The 0.4-eV difference between the two results was attributed to H-H repulsion effects. Additional calculations allowed a quantitative assessment of the hydrogen-hydrogen interaction energy $U$ in the vacancy; it was found that $U \approx 0.11$ eV. We note that instead of choosing H at BC as the final state, one also can choose H in free space as the reference; this leads to the energy values shown in Fig. 2.

Another way of defining an energy for the Si—H bond is to assume that one starts from crystalline silicon and a hydrogen atom in free space and

that the energy to create a dangling bond needs to be taken into account; this defines a *formation energy*. It is possible to extract a formation energy for an "ideal" Si—H bond (meaning it is located at a dangling bond that is isolated from other dangling bonds, with no H-H repulsion); the result is −2.17 eV (Van de Walle and Street, 1994). This value is very close to the calculated value for the $SiH_4$ molecule (−2.22 eV), expressed with respect to bulk Si and a free H atom (see Fig. 2). This concept of a formation energy will be discussed in more detail in Section II.6.a.

It should be noted that all values of binding energies and formation energies mentioned here assume that both the dangling bond and the intestitial H atom occur in the neutral charge state; starting from these values, the corresponding values for other charge states can be derived if the energy levels of the dangling bond and of the interstitial H are known.

It is also interesting to investigate whether strain in the backbonds affects the strength of the Si—H bond. Strain effects might be important in the case of an amorphous network. To simulate strain, the three Si atoms to which the Si atom with the dangling bond is bonded were moved outward. The displacement was chosen to be in the plane of these three atoms and had a magnitude of 0.13 Å, representing a sizable strain (5% of the bond length). It was found (Van de Walle and Street, 1994) that the binding energy was only 0.05 eV smaller than in the unstrained case, leading to the conclusion that strain effects have only a modest influence on the binding energy of the Si—H bond.

Finally, I discuss the phenomenon of hydrogen exchange at Si—H bonds. Various experiments have shown that this exchange can proceed with very low energy barriers; one way to investigate the exchange is to monitor substitution of hydrogen by deuterium (Street, 1987). Tuttle *et al.* (1999) have examined the hydrogen exchange mechanism at a Si—H bond. Initially, one hydrogen atom is bound at the Si—H bond, and the second H approaches it as an interstitial atom. In a first step, this second atom assumes a BC configuration in a Si—Si bond adjacent to the dangling bond; this configuration is only 0.15 eV higher in energy than the configuration where hydrogen sits in a BC site far from the Si—H bond. In a second step, the two H atoms exchange places, a process that can proceed with a barrier of less than 0.2 eV. A detailed examination of this process reveals intermediate formation of an $SiH_2$-like complex. The overall low barriers for this process are in agreement with the experimental results of Branz *et al.* (1993) and Kemp and Branz (1995).

### *b. Si—H Bonds Calculated in an Amorphous Environment*

Various simulations have addressed the atomic and electronic structure of Si—H bonds in an amorphous environment. Nelson *et al.* (1988) studied

the effect of removing hydrogen atoms on the vibrational and electronic properties of *a*-Si:H using peudopotential-density-functional calculations and random-network models consisting of 54 Si atoms and 6 H. They found that dangling-bond states have an average energy 0.2 eV above the valence band, which is lower than indicated by experiment; however, the effect of LDA bandgap errors was not discussed. The Si—H bonding states were located 5.0 and 7.5 eV below the top of the valence band. For a simpler model, consisting of a hydrogenated vacancy, DiVincenzo *et al.* (1983) had found Si—H bonding character for states 4.5 eV below the valence band.

Additional information about binding of H to Si dangling bonds will be discussed in Section II.5.

### c. *Dissociation Mechanisms of Si—H Bonds*

Several pathways can be considered for dissociation of Si—H bonds (Van de Walle and Street, 1994). The H atom can move along the direction of the Si—H bond away from the Si atom (Fig. 5); however, this is unlikely to be the most favorable path for two reasons: (1) the initial rise in energy in that direction is high, as indicated by the high vibrational frequency (around 2000 $cm^{-1}$) for the Si—H stretch mode, and (2) this path eventually leads

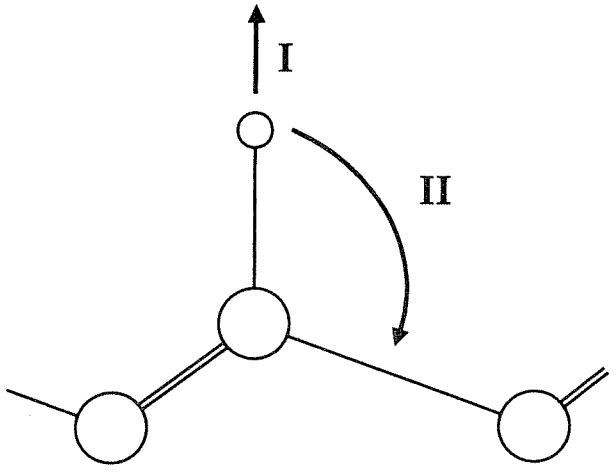


FIG. 5. Schematic representation (projected on a (110) plane) of a Si—H bond and the neighboring Si atoms. Si atoms are represented by large circles and the H atom by a small circle. Two paths for removing the H atom from the Si—H bond (leaving a dangling bond behind) are indicated; path *I* moves the H atom toward a tetrahedral interstitial site; path II moves the H atom toward a neighboring BC site. (From Van de Walle and Street, 1994.)

to a position of the H atom in the interstitial channel, which is not the lowest energy site for H in the neutral or positive charge state (in crystalline Si) (see Sec. I.2.a). Both these arguments actually favor a path (path II in Fig. 5) in which the H atom stays at an approximately constant distance from the Si atom to which it is bound: (1) the barrier in that direction is much lower, as indicated by the vibrational frequency (around 700 $cm^{-1}$) for the Si—H wagging mode, and (2) this path leads to a H position near the BC site, which is the stable site for $H^0$ (and also for $H^+$) in crystalline Si.

The intermediate state, with the H atom in a BC site next to the dangling bond, is 1.5 eV higher in energy than the Si—H bond, to be compared with the 2.5 eV it costs to remove the H to a position far away from the dangling bond (Van de Walle and Street, 1994). Alternatively, the intermediate state may involve H in an AB site (Tuttle and Van de Walle, 1999). Even before the H atom reaches this intermediate position, however, two energy levels are introduced into the bandgap (near the valence band and near the conduction band), enabling the complex to capture carriers; after changing charge state, there is virtually no barrier to further dissociation. Experimentally, the involvement of carriers in the migration of H in *a*-Si:H was established by Santos and Johnson (1993); it was found that the motion of H is strongly suppressed in a depletion region under reverse bias, where no free carriers are available. The barrier for dissociation therefore can be reduced significantly in doped material or in the presence of light-induced carriers. An interesting application of the features of this dissociation path will be discussed in Section II.6.

### 3. HYDROGEN INTERACTIONS WITH OVERCOORDINATION DEFECTS

When discussing hydrogen passivation of deep levels in crystalline and amorphous silicon, it is often assumed that the deep levels are due to dangling bonds. Indeed, this type of interaction can be monitored explicitly, e.g., with electron spin resonance (ESR), which produces a characteristic signature of the dangling bond. However, one should not focus only on undercoordination defects (dangling bonds) but also contemplate the possible existence of overcoordination defects. Indeed, in crystalline Si it has been accepted for some time that vacancies are not the only type of intrinsic defect to play a role. The early first-principles calculations of Bar-Yam and Joannopoulos (1984) and Car *et al.* (1985) already indicated that self-interstitials have formation energies comparable with those of vacancies; this result has been confirmed by more recent state-of-the-art investigations by Blöchl *et al.* (1993).

In amorphous silicon, too, overcoordination defects (interstitials) may

occur, in addition to undercoordinated atoms, as pointed out by Pantelides (1986). In crystalline silicon, the self-interstitials are known to play a role in self-diffusion (Blöchl *et al.*, 1993), impurity diffusion (Cowern *et al.*, 1994; Eaglesham *et al.*, 1994), surface reconstructions (Dabrowski *et al.*, 1994), planar interstitial defects (Kohyama and Takeda, 1992), and dislocation nucleation (Tan, 1981). However, because of their high mobility, isolated silicon self-interstitials have never been observed directly (Watkins, 1991). Despite the accepted importance of silicon self-interstitials and of hydrogen interactions with defects in silicon, the interaction between self-interstitials and hydrogen has been addressed only recently, in computational work by Jones *et al.* (see Bech Nielsen *et al.*, 1995) and by Van de Walle and Neugebauer (1995). Experimental investigations were performed by Bech Nielsen *et al.* (1995).

Complexes consisting of one or two H atoms and a Si self-interstitial were investigated using first-principles calculations, addressing atomic structure, electronic structure, and vibrational frequencies (Van de Walle and Neugebauer, 1995). It was found that hydrogen interacts strongly with self-interstitials; while the calculated binding energy is smaller than for H interacting with a vacancy, it is large enough for the complexes to be stable at room temperature.

The lowest-energy structure of the isolated Si self-interstitial ($Si_I$), in the neutral charge state, consists of a pair of Si atoms, oriented in the $\langle 110 \rangle$ direction, sharing a substitutional lattice site (a split-interstitial configuration); the calculated geometry is illustrated in Fig. 6, showing a small cluster of atoms near the core of the defect. In the perfect crystal, this cluster would contain seven atoms, five of which lie in a $(\bar{1}10)$ plane (forming the characteristic zigzag chain) and two of which lie in a perpendicular (110) plane. One also can think of the cluster as consisting of a central atom surrounded by four nearest neighbors and two additional second-nearest neighbors. In the case of the self-interstitial, the lattice location at the center of the cluster is now shared by two atoms. Figure 6 shows the cluster viewed along the $[\bar{1}10]$ direction.

The structure of a complex between the self-interstitial and one H atom, as obtained by Van de Walle and Neugebauer (1995), is shown in Fig. 7. This configuration was found to have the lowest energy among many potential candidates obtained by adding the H atom (in various positions) to some of the basic configurations of the self-interstitial, including the $\langle 110 \rangle$ and $\langle 100 \rangle$ split interstitials and the tetrahedral interstitial site. The most stable configuration has all atoms at the core of the defect lying in the $(\bar{1}10)$ plane, with the Si atoms distorted from their positions in the $\langle 110 \rangle$ split interstitial (see Fig. 7). The calculated vibrational frequency for the stretch mode of the Si—H bond is 1870 $cm^{-1}$, slightly smaller than the values in $SiH_4$ or for Si—H bonds on an Si surface (Van de Walle, 1994).

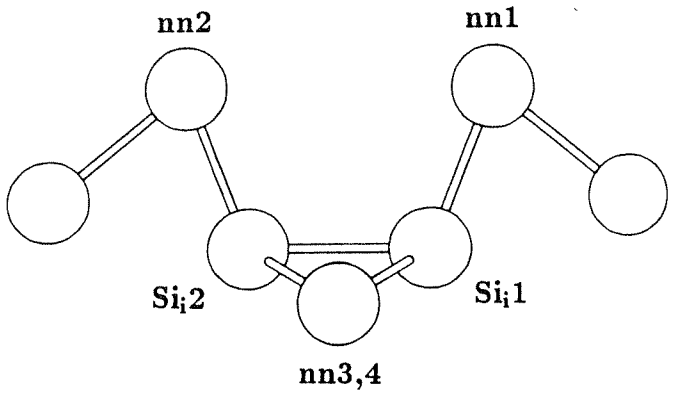


FIG. 6. Schematic representation of a cluster of Si atoms containing a Si self-interstitial in the split-interstitial configuration, oriented in the [110] direction. In the perfect crystal, the cluster consists of a central Si atom, surrounded by its four nearest neighbors, as well as two additional second-nearest neighbors. Now the central lattice site is shared by two Si atoms, labeled $Si_i1$ and $Si_i2$. The nearest neighbors nn1 and nn2, as well as the atoms to which they are bound, also lie in the plane of the figure. Nearest neighbors nn3 and nn4 lie in a plane perpendicular to the plane of the figure. (From Van de Walle and Neugebauer, 1995.)

The calculated binding energy, expressed with respect to an isolated H interstitial (at the BC site), is 1.34 eV. This is smaller than the binding energy for H to a dangling bond (2.50 eV) but larger than, for example, the binding energy of H to shallow impurities such as B or P (Van de Walle and Street, 1994). The electronic structure of the defect indicates that it is amphoteric

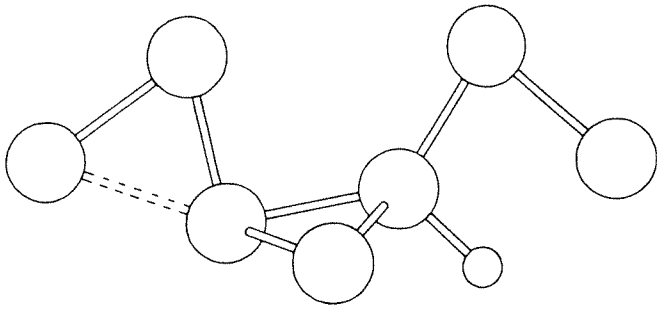

FIG. 7. Schematic representation of a cluster of Si atoms containing a complex between a Si self-interstitial and a single H atom. The Si atoms at the core of the defect are in positions that are distorted from the self-interstitial configuration illustrated in Fig. 6. (From Van de Walle and Neugebauer, 1995.)

in nature, with the acceptor level (transition level for the 0/− transition) located less than 0.1 eV above the donor level (the transition level for the +/0 transition) and both located around 0.4 eV above the valence band.

Complex formation between *two* H atoms and a Si self-interstitial also has been investigated (Van de Walle and Neugebauer, 1995). The structure of the complex is illustrated in Fig. 8. Now the two Si atoms at the core of the interstitial have twisted out of the $(\bar{1}10)$ plane. The bond between the two Si atoms attached to H is oriented 28° off $\langle 110 \rangle$ and only 17° off $\langle 100 \rangle$, so the configuration is actually closer to a $\langle 100 \rangle$ interstitial (Jones, 1997). The distortion allows these atoms to assume nominally fourfold coordination; i.e., they are bonded to four other atoms (three Si and one H), although the bond angles are significantly distorted (by as much as 35°) from the tetrahedral bond angle of 109°. The calculated vibrational frequency for the Si—H stretch mode is 1915 $cm^{-1}$. The calculated binding energy of this complex is 2.40 eV per H atom (with respect to the free H atom), essentially the same as for the complex with one H atom. The complex with two hydrogens has no levels in the bandgap, consistent with all the bonds being satisfied. These results for the atomic and electronic structure indicate that a single self-interstitial is unlikely to bind more than two H atoms.

Bech Nielsen *et al.* (1995) reported pseudopotential-density-functional calculations for complexes between the self-interstitial and two hydrogens. Their calculated structure is close to the one obtained by Van de Walle and Neugebauer (1995), with the bond between the two Si atoms attached to H 30° off $\langle 110 \rangle$ and only 12° off $\langle 100 \rangle$ (Jones, 1997). The calculated vibrational frequencies reported by Bech Nielsen *et al.* (1995) for the complex are 2106 and 2107 $cm^{-1}$. Bech Nielsen *et al.* (1995) also carried out vibrational spectroscopy for hydrogen interacting with native defects in *c*-Si and tentatively ascribed two modes, at 1987 and 1990 $cm^{-1}$ to a $\langle 100 \rangle$ split interstitial saturated by two hydrogens. These values are somewhat closer to those calculated by Van de Walle and Neugebauer (1995), lending additional support to the assignment to a structure based on a $\langle 110 \rangle$ split interstitial.

The structures described here were derived for a crystalline environment; still, the general features also may apply to overcoordination defects in *a*-Si. First-principles calculations of Si—H bonds in amorphous networks by Tuttle and Adams (1998) included one example where removing a H atom from a Si—H bond leaves a fivefold coordinated Si atom behind. The binding energy in this case was calculated to be 1.5 eV, referenced to H at the BC in *c*-Si; this value is in good agreement with the results quoted earlier for H binding to a self-interstitial in *c*-Si. I also note that the calculated vibrational frequencies for the Si—H stretch modes, which are somewhat lower than for Si—H bonds at dangling bonds, could help explain why the

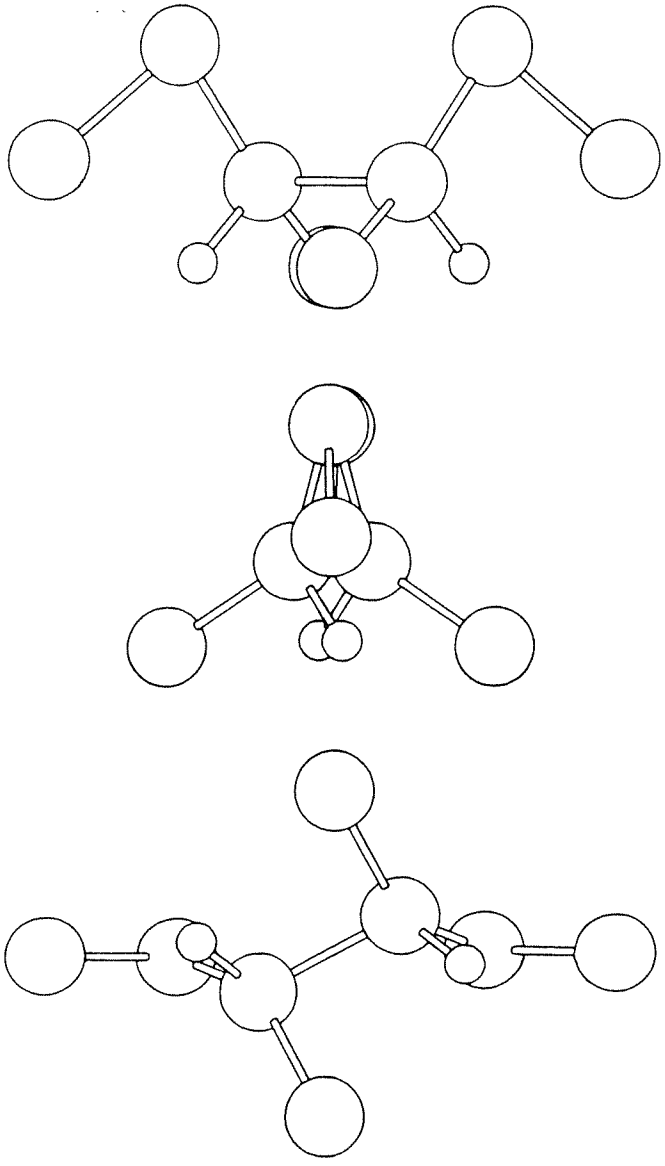

FIG. 8. Schematic representation of a cluster of Si atoms containing a complex between a Si self-interstitial and two H atoms. The Si atoms at the core of the defect are in positions that are distorted from the self-interstitial configuration illustrated in Fig. 6. In order to show the distortion out of the $(\bar{1}10)$ plane, the cluster is viewed from three different directions: along the $[\bar{1}10]$ direction (top), along the $[1\bar{1}0]$ direction (center), as well as along the [001] direction (bottom). (From Van de Walle and Neugebauer, 1995.)

absorption band corresponding to Si—H stretch modes extends to lower frequencies. The electrical activity of the complex described earlier is also relevant for understanding deep levels in *a*-Si. Furthermore, this complex may be a candidate for the H-induced acceptors observed by Nickel *et al.* (1995) in polycrystalline Si, as described in Section III.4.

## 4. HYDROGEN INTERACTIONS WITH WEAK Si—Si BONDS

Li and Biswas (1995a, 1995b) used a tight-binding molecular dynamic study (see Sec. I.3.d) to derive formation energies for insertion of hydrogen into weak Si—Si bonds. First, they generated a model of *a*-Si:H containing 272 atoms with periodic boundary conditions, containing both SiH and $SiH_2$ species. They calculated the formation energy of the reaction described by Eq. (1) at more than 70 different sites. In order to increase the likelihood of weak-bond occurrence, they systematically created strained *a*-Si:H configurations by dilating the supercells. Their results are shown in Fig. 9.

They arrived at the conclusion that the defect formation energy scales almost linearly with the bond-length deviation:

$$E = E_0 - \alpha \Delta R \tag{2}$$

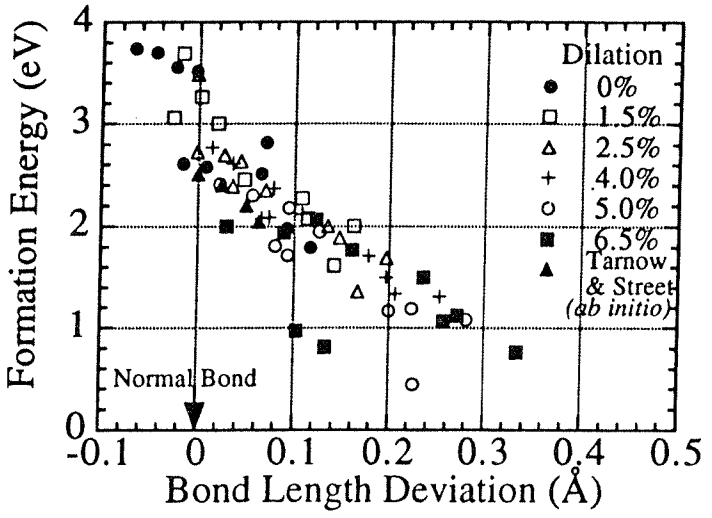


FIG. 9. Formation energy for the reaction described by Eq. (1) as a function of the Si—Si bond-length deviation. To enhance the likelihood of weak-bond occurrence, calculations were performed in cells with varying amounts of dilation. First-principles results from Tarnow and Street (1992) are also included. (From Li and Biswas, 1995a.)

where $\Delta R$ is the deviation of the Si—Si bond length from the average value. The calculations of Li and Biswas (1995a, 1995b) produced $E_0 = 2.5$ eV and $\alpha \approx 6.3$ eV/Å. In Section III.3 I will discuss calculations (Van de Walle and Nickel, 1995) that were performed in a crystalline environment and produced a value for $\alpha$ between 4 and 5 eV/Å. The agreement is quite reasonable, with the larger value for *a*-Si:H indicative of an environment in which the atoms can relax more easily to accommodate the hydrogen-induced defect. It is possible, however, that the larger value of $\alpha$ obtained by Li and Biswas (1995a) is affected to some extent by their procedure, which involves dilation of the *a*-Si:H model (Tuttle and Adams, 1998).

## 5. SIMULATIONS OF AMORPHOUS NETWORKS

In this section I discuss computations for hydrogenated amorphous networks, which provide information about larger-scale atomic structure and/or energetics of the Si—H interactions.

Buda *et al.* (1991, 1992) performed first-principles molecular dynamics simulations, based on the pseudopotential-density-functional method and the Car-Parrinello approach (see Sec. I.3.a), for supercells containing 64 Si atoms and 8 H atoms. They obtained the amorphous structure by cooling from the melt; the cooling rate is inevitably much faster than in real experiments. Only monohydride groups occurred in the sample, supporting the idea that $SiH_2$ and other polyhydride groups have a low probability of occurring. A pronounced peak was found in the H-H pair correlation function around 2.5 Å, indicating a tendency for H to cluster.

Lee and Chang (1994) performed first-principles molecular dynamics simulations based on the density-functional-pseudopotential approach for supercells containing 64 atoms. Rather than using a fast quench from a liquid phase, they followed the procedure of Drabold *et al.* (1990), in which disordered networks are produced by a brief heating of *c*-Si, characterized by an incompletely melted sample. Their structural parameters were in reasonable agreement with experiment. Lee and Chang (1994) found that their amorphous model contained more dangling bonds than previously generated samples from liquid-quench simulations; this agrees with an assessment by Tuttle and Adams (1996) to be discussed below. Lee and Chang (1994) analyzed the electronic structure of the defects and found that the wave function of the midgap state has *p*-like character and is more localized on a threefold coordinated site than on a fivefold coordinated defect, in agreement with ESR (electron spin resonance) data.

Tuttle and Adams (1996) created a 242-atom model of *a*-Si:H using the approximate first-principles-pseudopotential approach based on the Harris

functional (see Sec. I.3.b). They carried out a critical assessment of models derived from molecular dynamics; models produced from a liquid tend to be overcoordinated, whereas models produced from a crystal tend to lack disorder. They observed clustering of monohydrides in two distinct fashions: on the one hand, microclusters of two to four H, and on the other hand, H passivation of larger cavities.

Fedders and Drabold (1993) and Fedders (1995) used the approximate first-principles method described in Section I.3.b to create and study amorphous networks in supercells containing 62 Si atoms and varying numbers of H atoms. The cells contained 0, 1, or 2 well-localized defects. Fedders (1995) obtained properties of hydrogen configurations, in different charge states, for H at dangling bonds, in BC sites, and in other interstitial sites. The main result was a large spread of energies for a given type of defect; both H at BC and H at a dangling bond exhibited a spread of about 1 eV in binding energies, accompanied by considerable variations in the structural properties. This led Fedders to the conclusion that the distinction between BC hydrogen and a dangling bond plus a Si—H bond was not clear-cut.

More recently, first-principles results by Tuttle and Adams (1998) have contradicted the conclusions of Fedders (1995). For their study, Tuttle and Adams used self-consistent pseudopotential-density-functional theory on the *a*-Si:H model created by Guttman (1981) and Guttman and Fong (1982). They examined the energies of H inserted into Si—Si bonds and found the BC position to have an average energy 0.2 eV lower than BC in *c*-Si. For H bound in Si—H bonds, they found energies between 1.7 and 2.1 eV below H at BC in *c*-Si; the higher-lying energies are due to H-H interactions. They also identified configurations where removal of a H atom leads to reconstruction of a Si—Si bond; these Si—H bonds have energies in the range of 1.2–1.3 eV below H at BC in *c*-Si. The range over which the energies of the "shallow" and "deep" traps vary is much smaller than found by Fedders (1995); Tuttle and Adams attributed the differences with the work of Fedders (1995) to the more approximate nature of Fedder's calculational method.

Tuttle and Adams (1997) also examined the geometric and vibrational properties of clusters formed by hydrogen passivating a weak bond. They performed molecular-dynamics simulations for four different models of *a*-Si:H: one containing 54 atoms (Guttman, 1981; Guttman and Fong, 1982), one containing 68 atoms (Fedders and Drabold, 1993), one with 72 atoms (Buda *et al.*, 1991), and finally a 242-atom model developed by Tuttle and Adams themselves (1996). They proposed that these complexes are responsible for hydrogen clustering in disordered Si.

Finally, I note that the simulations of Fedders and Drabold (1996)

revealed the existence of a quasi-continuous manifold of nearly degenerate and conformationally distinct metastable minima that are accessible to each other at moderate simulation temperatures. They suggested that these are the states associated with two-level systems. Low-energy excitations were observed, such as elastic modes with anomalously low frequencies ("floppy modes").

## 6. HYDROGEN DIFFUSION AND METASTABILITY — DISCUSSION

### *a. Quantifying Energy Levels*

Now that we have accumulated a host of quantitative information on configurations and energetics of H in *a*-Si:H, we can return to the issues raised in Section II.1 and address the identification of the energies depicted in Fig. 4. One approach was given by Van de Walle and Street (1995), based on energy values included in Fig. 2. The zero of energy in that figure was chosen to correspond to the energy of a neutral H atom in free space. The level at $-3.55$ eV corresponds to the energy required to remove a hydrogen atom from an ideal Si—H bond, leaving a dangling bond behind. The theoretical definition of the level indicates that it is equivalent to the $E_{\mathrm{Si-H}}$ level in Fig. 4.

A key energy value (Van de Walle and Street, 1995) is the *formation energy* of a Si—H bond, referenced to bulk Si. This energy is listed in Fig. 2 at $-2.17$ eV and is derived by calculating the energy for the Si—H bond embedded in a Si environment and subtracting the energy of the H atom and of the Si atoms, assuming that all Si atoms are part of a bulk environment. Van de Walle and Street (1995) argued that this value is connected to the hydrogen chemical potential $\mu_{\mathrm{H}}$. The difference with the energy at $-3.55$ eV discussed earlier is that one includes the formation of a dangling bond, whereas the other does not. Note that the difference between the binding energy and the formation energy is $-2.17-(-3.55)=1.38$ eV; this value constitutes an estimate for the formation energy of a dangling bond in *c*-Si.

To understand the connection between the formation energy of Si—H bonds and $\mu_{\mathrm{H}}$, we need to describe the significance of $\mu_{\mathrm{H}}$ in the case of *a*-Si:H. First of all, it is important to realize that $\mu_{\mathrm{H}}$ should *not* be located at $E_{\mathrm{Si-H}}$, which is the energy level corresponding to Si—H bonds. Instead, the chemical potential is located at an energy that corresponds to a minimum in the density of states. The density of states illustrated in Fig. 4b has contributions from two types of states: Around $E_{\mathrm{Si-H}}$ there is a distribution of Si—H bond energies; at higher energies we find a distribution

of energies for interstitial hydrogen associated with distortions in weak Si—Si bonds. Hydrogen can move between these two types of configurations: Starting from a Si—H bond, hydrogen can move into a weak Si—Si bond, leaving a dangling bond behind, as described by the reaction in Eq. (1). The Si—H—Si bond can, in turn, convert to a Si—H bond plus a dangling bond; this does not affect the discussion here.

The chemical potential $\mu_H$ has to be located at a minimum in the density of states, between the weak-bond and Si—H bond levels. This follows from an energy-minimization argument: If $\mu_H$ were higher, a larger number of H atoms in weak Si—Si bonds would be formed, costing energy; if $\mu_H$ were lower, additional H atoms would be removed from Si—H bonds, creating dangling bonds, which also costs energy. The minimum-energy situation therefore occurs for $\mu_H$ located at the minimum in the density of states. This location is consistent with the observation that *a*-Si:H contains a relatively low number of dangling bonds; most bonds in the structure are satisfied, either because they are part of Si—Si bonds or by forming Si—H bonds. Furthermore, this location of $\mu_H$ corresponds to the condition that the formation energy of a Si dangling bond in *a*-Si:H is zero. Indeed, $\mu_H$ lies at the level where the formation energy of a Si—H—Si bond is equal to the formation energy of a Si—H bond; if we associate an energy with each of the terms in Eq. (1), this leads to the condition that the formation energy of the Si dangling bond in *a*-Si:H must be zero.

This discussion about $\mu_H$ immediately provides a connection with Fig. 2. The arguments in the preceding paragraphs show that the hydrogen chemical potential $\mu_H$ corresponds to the level where the formation energy of the dangling bond in *a*-Si:H is zero. We thus find that $\mu_H$ should be identified with the level corresponding to the formation energy of a Si—H bond, which was calculated to be at $-2.17$ eV. This allows derivation of a theoretical value for the activation energy $E_A$ in Fig. 4: $E_A = E_S - \mu_H = (E_S - E_{BC}) + (E_{BC} - \mu_H) = [0.2 \cdots 0.5] + (1.12) = [1.32 \cdots 1.62]$ eV, where the range takes into account the uncertainty in $E_S - E_{BC}$. This value agrees well with experimental numbers for the diffusion activation energy $E_A$.

The formation energy of the Si—H bond is actually very close to the calculated formation energy of the Si—H bond on the Si(111) surface ($-2.14$ eV), as well as to the formation energy of $SiH_4$ ($-2.22$ eV), all expressed with respect to Si bulk (see Fig. 2). The similarity of these values indicates that there is no single microscopic structure that gives rise to this energy value; the key is that no energy cost needs to be paid for breaking any Si—Si bonds. Specific microscopic "implementations" also could include, for example, the extended $H_2^*$-based defects proposed by Zhang and Jackson (1991). The consistency of all these values strengthens our identification of this level with the hydrogen chemical potential. Placing $\mu_H$ at

$-2.17$ eV is also in good agreement with a rough estimate made by Street (1991c) based on an entirely different approach.

One remaining problem with the assignment of energy levels proposed by Van de Walle and Street (1995) is that the energy difference between $\mu_H$ and $E_{Si-H}$ becomes equal to $-2.17-(-3.55)=1.38$ eV, i.e., the formation energy of a dangling bond in *c*-Si. This value is unphysically large for *a*-Si for two reasons: (1) In order for the assumption of thermal equilibrium to be valid, hydrogen needs to be able to redistribute among the various states at the temperatures of interest; an energy of 1.38 eV would be too large to allow exchange of hydrogen between Si—H bonds and the chemical potential at typical diffusion temperatures. (2) The dangling-bond creation process in *a*-Si involves excitation of a H atom out of an Si—H bond, which once again would cost 1.38 eV; however, experimental observations give a value below 0.5 eV (Street and Winer, 1989).

Both concerns can be addressed by establishing that the $E_{Si-H}$ level is *higher* in *a*-Si than in *c*-Si. Indeed, explicit simulations for Si—H bonds in amorphous networks (see, e.g., Tuttle and Adams, 1998) show that the Si—H bond energies can be significantly higher than the value for H at an ideal, isolated dangling bond due to hydrogen clustering and H-H repulsion effects. In addition, mechanisms that facilitate the interchange between states at $E_{Si-H}$ and $\mu_H$ can be invoked. For instance, exchange of diffusing H atoms with H bonded in Si—H atoms may occur with lower activation barriers than needed for excitation of a single H out of an Si—H bond; evidence for such a mechanism was found in experiments where deuterium was exchanged with hydrogen (Street, 1987), as discussed in Section II.2.a. Finally, the barrier for dissociation of a Si—H bond may be reduced significantly in the presence of free carriers (see Sec. II.2.c).

### *b. Explicit Calculation of Energy Distributions*

Li and Biswas (1996) used the formation energies they obtained for weak Si—Si bonds (see Sec. II.4, Eq. 2) to derive an energy distribution for the formation energy of metastable defects under the assumption of a Gaussian distribution of the bond length. This allowed them to obtain a thermal equilibrium defect density, as well as a light-induced defect density, using a rate equation. Their calculated distribution of formation energies is shown in Fig. 10. This distribution depends on the value of $\alpha$ derived by Li and Biswas (1995a) (see Sec. II.4); if $\alpha$ is overestimated, as argued by Tuttle and Adams (1998), the distributions may be affected.

Li and Biswas (1996) also used their calculated energy distribution to examine the annealing dynamics of the defects. They found that (except at

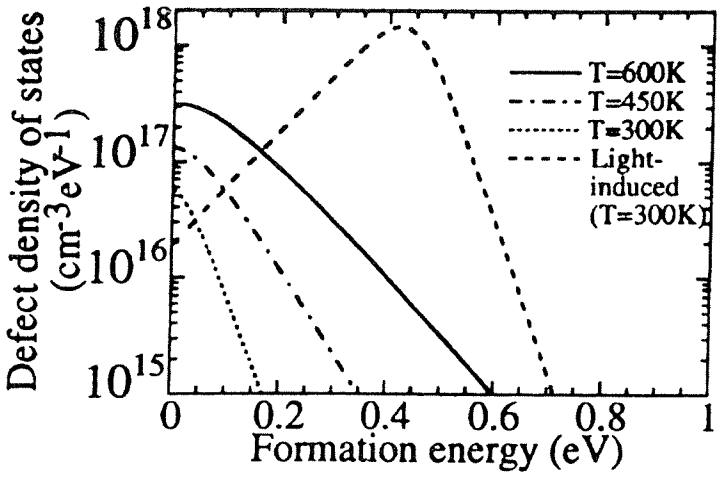


FIG. 10. Distributions of formation energies for thermal equilibrium and for light-induced defects. (Reprinted with permission from Li and Biswas, 1996. Copyright © 1996 American Institute of Physics.)

long times) the relaxation curves are well fit by a stretched exponential, in agreement with experiment (Kakalios *et al.*, 1987). An alternative, simple explanation for stretched-exponential-type relaxations was proposed recently (Van de Walle, 1996a, 1996b). This model is based on a description of the release and retrapping of hydrogen at trap sites with a *single* energy level; it was found that this model provides a fit to experimental data that is at least as good as the traditional stretched exponential, without requiring a distribution of trap energies. This finding indicates that a stretched-exponential-like relaxation is not necessarily indicative of the presence of a distribution of trap energies.

### c. *Models for Metastability*

Jones and Lister (1990) (see also Jones, 1991) performed first-principles pseudopotential calculations, in a cluster approach, to study H in various positions in *c*-Si, including configurations where the Si—Si bond was stretched. They found that as the Si—Si distance exceeds 3.8 Å, a transition takes place from the neutral symmetric BC configuration to a configuration with a Si—H bond plus a dangling bond. The positively charged BC center was found to be more stable.

Jones and Lister (1990) found that metastable states with an energy as low as 0.2 eV can form if the Si—Si bond is prestrained by 40%. They

suggested that the SW effect occurs as follows: Upon illumination, electron-hole pairs are created at strained Si—Si bonds ($\sim$20% strain), which are consequently weakened further ($>$40%), enabling spontaneous hydrogen migration into them before electron-hole recombination occurs. Alternatively, electron-hole pairs are created at 40% strained bonds, and nonradiative recombination promotes H migration over the barrier into the bond center. Jones and Lister acknowledged that the density of strained bonds required for this mechanism to explain the experimental observations would exceed the equilibrium density; they suggested the strained bonds would be introduced athermally during the deposition process.

An alternative model was proposed by Biswas *et al.* (1991). These authors identified a bridge-bonded hydrogen interstitial as the initial or annealed state; this configuration consists of a hydrogen in a three-center bond between two Si atoms at a distance of about 3.2 Å. In the light-soaked state, the Si—Si separation increases, and the hydrogen forms a Si—H bond with one of the Si atoms, leaving a dangling bond on the other Si. One problem with this model is that the initial state is already electrically active.

Jackson (1990) suggested that two-hydrogen-atom complexes were involved in the metastability. These neutral complexes, the so-called $H_2^*$ (Chang and Chadi, 1989; see Sec. I.2.e), consist of one H in a BC-like position and another H in an AB position. The complex can dissociate either thermally or through light-induced carriers into isolated atomic H configurations that diffuse rapidly to other weak Si—Si bond sites, creating midgap defects. Annealing occurs when these isolated H atoms form complexes either with the same or different H atoms. This proposal was backed up by first-principles calculations by Zhang *et al.* (1990), which demonstrated an explicit reaction pathway of carrier-induced changes through dissociation of paried-H complexes. The complex was shown to dissociate through the capture of charge carriers, with barriers that were found to be in agreement with the experimentally observed activation energies for single-carrier defect creation in *a*-Si:H.

Finally, I note that Li and Biswas (1996) recently used their tight-binding total-energy calculations to describe the changes in local structure following either electron or hole capture by a neutral dangling bond. They found significant changes in bond angles (by up to 10°) and displacements of nearest-neighbor Si and nearby H atoms (by more than 0.2 Å). Structural relaxations around a dangling-bond site, as a function of charge state, were investigated previously in a crystalline environment by Northrup (1989). The molecular dynamics simulations of Li and Biswas (1996) showed these relaxations to be fast, probably happening on a time scale less than 1 ms. These results do not support the suggestion that experimentally observed anomalously slow relaxations are associated with charge-state changes of dangling bonds (Cohen *et al.*, 1992).

## 7. HYDROGEN VERSUS DEUTERIUM FOR PASSIVATION OF DANGLING BONDS

Recently, some very exciting results were published on the different characteristics of hydrogen and deuterium (D) for passivation of Si dangling bonds. The phenomena were first studied in the context of passivation of dangling bonds on Si surfaces; specifically, the Si(100)-(2 × 1) surface can be passivated perfectly by hydrogen (or deuterium). It was demonstrated that desorption of hydrogen from this surface can be achieved, with atomic resolution, by irradiation with electrons emitted from a scanning tunneling microscope (STM) tip (Lyding *et al.*, 1994). When the experiment was repeated with deuterium (Avouris *et al.*, 1996a), a very strong isotope effect was observed; the deuterium desorption yield was much lower (up to 2 orders of magnitude) than the hydrogen desorption yield.

Lyding *et al.* (1996) built on these observations to conduct an experiment in which the difference between H and D was studied in the context of passivation of defects at the $Si/SiO_2$ interface. This interface lies at the heart of Si metal-oxide-semiconductor (MOS) transistor technology. The interface exhibits a high degree of perfection, but any remaining defects (usually considered to be dangling bonds) can be passivated by hydrogen, which is accomplished in an intentional hydrogenation during processing. Unfortunately, some degradation occurs over time, mostly due to hot-electron effects. Lyding *et al.* (1996) observed significant improvements in the lifetime of (MOS) transistors when deuterium, rather than hydrogen, was incorporated at the $Si/SiO_2$ interface. Similarly to the surface desorption experiments, this indicates that the Si—D bond is more resistant to hot-electron excitation than the Si—H bond.

At first sight, it is very difficult to understand why the mass difference between H and D should cause such a large difference. From an electronic point of view, the isotopes are equivalent, and the static electronic structure of the Si—H and Si—D bonds is identical. The difference therefore must be attributed to dynamics—but it is hard to come up with an explanation that yields such a remarkable difference in desorption rates (up to 2 orders of magnitude). For instance, one can invoke the difference in zero-point energies between the Si—H and the Si—D bond; however, this difference is on the order of 0.1 eV, whereas the dissociation barrier that needs to be overcome is on the order of several electronvolts; hence the small difference in zero-point energies has a negligible effect on tunneling rates, etc. Various other theoretical approaches have been suggested (Shen *et al.*, 1995; Avouris *et al.*, 1996b). Recently, a mechanism was proposed (Van de Walle and Jackson, 1996) that builds on these theoretical descriptions but proposes a specific pathway for the dissociation of Si—H and Si—D bonds, providing a natural explanation for the difference in dissociation rates.

It has been proposed that (at least in the low-voltage regime) the dissociation of Si—H bonds from Si(100) proceeds via a multiple-vibrational excitation by tunneling electrons (Shen *et al.*, 1995)—a mechanism that would apply both to desorption from the surface and to the $Si/SiO_2$ interface. Electrons excite Si—H vibrational transitions with a rate proportional to the tunneling current. The extent to which vibrational energy can be stored in the bond depends on the lifetime, i.e., on the rate at which energy is lost by coupling to phonons. Because the lifetime of H on Si is long (Guyot-Sionnest *et al.*, 1990, 1995), efficient vibrational excitation is expected. In the quantitative analysis by Shen *et al.* (1995) it was assumed that the vibrational energy is deposited in the *stretch* mode of the Si—H bond, which has a frequency around $2100\,cm^{-1}$. The same assumption is usually made implicitly in discussions of dissociation of Si—H bonds.

Van de Walle and Jackson (1996) pointed out that both the vibrational lifetime and carrier-enhanced dissociation mechanisms are most likely controlled by the Si—H *bending* modes, as discussed in Section II.2.c. The vibrational frequency of the bending mode for Si—H is around $650\,cm^{-1}$, and the estimated frequency for Si—D is around $460\,cm^{-1}$. This value is close to the frequency of bulk TO phonon states at the X point ($463\,cm^{-1}$) (Madelung, 1991). Therefore, one can expect the coupling of the Si—D bending mode to the Si bulk phonons to result in an efficient channel for deexcitation. While it is quite possible to reach a highly excited vibrational state in the case of Si—H, this will be more difficult for Si—D. Deuterium therefore should be much more resistant to STM-induced desorption and hot-electron-induced dissociation due to the relaxation of energy through the bending mode.

Furthermore, as discussed in Section II.2.c, the bending mode provides a likely pathway for dissociation in the presence of carriers. Two conclusions mentioned in Section II.2.c have direct consequences for the vibrational excitation mechanism: (1) In the bulk, the bending-mode pathway for dissociation of a single Si—H involves an intermediate metastable state with the H atom located adjacent to the dangling bond (from which H has been removed). The activation barrier to reach this intermediate state is 1.5 eV, which is 1 eV lower than the energy difference between the Si—H bond and an isolated interstitial H. In this intermediate state, the system has electrically active levels in the bandgap; on capture of a carrier, the charge state of the hydrogen can change, and subsequent dissociation will proceed with no additional barrier. (2) Even before this intermediate metastable state is reached, levels are introduced into the bandgap. When the displacement of H from its equilibrium position reaches about 0.8 Å, gap levels emerge from the conduction and the valence bands. Again, capture of carriers in a gap level results in immediate dissociation. The bending-mode excitation path-

way is therefore attractive because of the potential for carrier-enhanced dissociation and because the overlap of the Si—D bending-mode frequency with Si bulk phonons provides a natural explanation for its reduced dissociation rate.

It is tempting, of course, to suggest that the enhanced stability of Si—D compared with Si—H at Si surfaces and $Si/SiO_2$ interfaces also would apply to Si—D bonds in *a*-Si and could be used to address metastability and degradation problems. To my knowledge, no conclusive experiments on this issue have been performed. To observe an effect, it may be necessary to have most or all of the hydrogen in the sample replaced by deuterium; as long as any Si—H bonds are present, they may be the first to dissociate, leading to severe degradation even in the presence of deuterium. Further work in this area should be worthwhile.

## III. Hydrogen in Polycrystalline Silicon

### 1. GRAIN BOUNDARIES

The grain boundaries are the most distinguishing feature of polycrystalline silicon. Inside the grains, the material is essentially bulk crystalline silicon, and hydrogen will display its usual range of behaviors there, including fast diffusion, formation of $H_2$ molecules, passivation of shallow and deep levels, formation of platelets (Nickel *et al.*, 1996), etc. Near the grain boundaries, however, the structure of the material is qualitatively different, and new phenomena can be expected to occur. The grain boundary is a two-dimensional extended defect (Bourret, 1985). When two grains are joined at a boundary, there is a strong driving force for reconstruction (Queisser, 1983); however, some point defects remain, which have been detected by electron spin resonance (ESR) and identified as Si dangling bonds (Johnson *et al.*, 1982). In addition, shallow localized states occur that form band tails; these states have been attributed to strained Si—Si bonds (Jackson *et al.*, 1983).

Detailed microscopic information on the atomic structure of grain boundaries is only gradually becoming available. A small number of computational studies have been performed; the following overview is not intended to be exhaustive but mainly to highlight the main features I will be using here. Thomson and Chadi (1984) performed tight-binding calculations of a high-angle tilt boundary in Si; they found that no dangling bonds were present, illustrating the large degree of reconstruction that takes place. Some deviations in bond length and bond angle were found, however. Similar

conclusions were found by DiVincenzo *et al.* (1986) for a twin boundary in Si. More recently, Kohyama and Yamamoto (1994) performed semiempirical tight-binding calculations of twist boundaries in Si. They found that twist boundaries exhibit greater structural disorder and larger interfacial energies than tilt boundaries. The twist boundaries contain more coordination defects (dangling bonds or floating bonds) and also exhibit larger bond distortions (with bond-length deviations up to 10%). Recently, empirical-potential molecular-dynamics simulations produced the result that in thermodynamic equilibrium all high-energy grain boundaries are highly disordered, with a layer of about 5 Å around the boundary that is amorphous in nature (Keblinski *et al.*, 1997).

Detailed information has been obtained from first-principles studies for grain boundaries in Ge (Tarnow *et al.*, 1989, 1990). For the $\Sigma 5$ and $\Sigma 5^*$ twist boundaries, an *ab initio* molecular dynamics approach produced optimized geometries, for which the distribution of bond lengths was then examined. Atoms in the first layer near the boundary were found to exhibit nearest-neighbor bond lengths ranging from 2.2 Å to more than 2.8 Å; the equilibrium bond length in Ge is 2.45 Å. The distribution was asymmetric, with stretched bonds outnumbering compressed bonds.

In Section III.2 we will be particularly interested in the bond-length deviations that occur near grain boundaries. One may expect that bond distortions around dislocations bear some similarity to those around grain boundaries. I note that first-principles calculations also have been carried out for 90° partial dislocations in Si (Bigger *et al.*, 1992); one may expect that the features of the atomic geometry around dislocations bear some similarity to those around grain boundaries. The results of Bigger *et al.* (1992) indicate that, once again, there is a tendency for bonds to be stretched, by amounts that can exceed 5% of the bond length (i.e., larger than 0.1 Å).

I conclude that (1) coordination defects (such as dangling bonds) can occur near grain boundaries, although they seem to occur mostly near higher energy (e.g., twist) boundaries, and (2) deviations in bond length and bond angle are common near grain boundaries, with stretched bonds occurring more frequently than compressed bonds and distortions of up to 10% of the bond length.

## 2. HYDROGEN INTERACTIONS WITH GRAIN BOUNDARIES

It is well known that hydrogen can passivate deep levels associated with the grain boundaries in poly-Si. Unlike the *a*-Si case, where H is incorporated during growth, dangling-bond defects in poly-Si are passivated by

posthydrogenation at elevated temperatures. Exposure of poly-Si to monatomic hydrogen (from a remote plasma) at temperatures between 250 and 450°C leads to a decrease in the dangling-bond density as well as a reduction in the density of band-tail states (Johnson *et al.*, 1982; Jackson *et al.*, 1983). The details of the hydrogenation procedure can have a strong effect on the remaining spin density (Nickel *et al.*, 1993a, 1993b); for more specific information, see Section IV of Chap. 4 in this volume. The passivation effects due to hydrogen are probably quite similar to those in amorphous silicon, as discussed in Section II. Not surprisingly, light-induced metastability has been observed (Nickel *et al.*, 1993b), which has been associated with the interaction between hydrogen, dangling bonds, and strained Si—Si bonds.

One key experiment was performed on undoped samples that had been hydrogenated until the defect density saturated at a minimum value (Nickel *et al.*, 1994). It was found that annealing around 160°C followed by a quench to low temperature produced an enhancement in the conductivity. The enhancement was metastable and decayed with time. The temperature dependence of the decay rate indicated that the activation energy for the decay process is $E_A \approx 0.74$ eV. This activation energy allows for the metastable state to have a lifetime on the order of hours at room temperature. These observations are consistent with a model in which quenching leads to the trapping of H in an electrically active metastable state. The decay of the conductivity is then associated with the release of H from the metastable configuration. The H that is released from the traps returns to a lower-energy state (Fig. 11); this "reservoir" of H was found to have an energy 0.35 eV below that of the metastable state (Nickel *et al.*, 1994). The experimental aspects are described in more detail in Section V.2 of Chap. 4 in this volume. I will examine the microscopic nature of this metastable state in the next section.

## 3. HYDROGEN-INDUCED GENERATION OF DONOR-LIKE METASTABLE DEFECTS

In the Introduction (Sec. I.2) I discussed the main features of the interactions between H and Si. The configurations that have energies in the relevant range are shown in Fig. 11 (configurations with energies below −2.15 eV are not included in the figure). An isolated, neutral H interstitial in Si resides at the BC site, with an energy 1.05 eV below the energy of H in free space. In this configuration, hydrogen acts as a donor, with a level about 0.2 eV below the conduction band (Bech Nielsen, 1991; Johnson *et al.*, 1994; Van de Walle *et al.*, 1989). The activation energy $E_A$ mentioned earlier

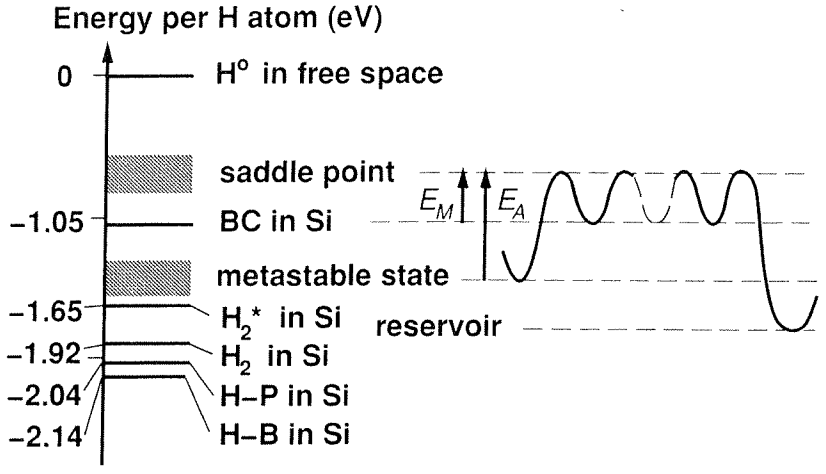


FIG. 11. Schematic diagram depicting first-principles energies of various configurations of hydrogen in silicon, as well as energy as a function of position. The saddle point for migration lies $E_M = 0.2 - 0.5$ eV above the level of H at BC. The activation energy $E_A \approx 0.74$ eV, obtained from the experiments by Nickel *et al.* (1994), is the energy difference between the metastable configuration and the saddle point. The energy of the metastable state therefore lies between $-1.6$ and $-1.3$ eV. (From Van de Walle and Nickel, 1995.)

corresponds to the energy difference between the metastable state and the saddle point of the migration path of an interstitial H atom. This saddle point occurs at an energy $E_M$ above the level of the H interstitial at BC. The activation barrier for migration can be estimated to be between 0.2 and 0.5 eV, the lower number resulting from a first-principles calculation of an adiabatic energy surface (Van de Walle *et al.*, 1989) and the higher number from high-temperature diffusion experiments (Van Wieringen and Warmoltz, 1956). We thus find that the energy of the metastable state is between $-1.6$ and $-1.3$ eV.

Figure 11 shows that stability of most Si—H configurations is such that activation energies much higher than 0.74 eV would be required to release hydrogen. In fact, the only configuration that allows for hydrogen to escape at room temperature or below is that of an isolated interstitial H atom at BC. In crystalline Si, the stability of BC hydrogen has been derived from DLTS (deep-level transient spectroscopy) measurements. It was found that the BC configuration is only stable at temperatures below 100 K (Bech Nielsen, 1991). However, variations on the basic BC configuration are possible that provide a higher stability and lower the energy of this configuration to fall in the range of $-1.6$ to $-1.3$ eV. As discussed in Section I.2.a, the formation energy of the BC configuration involves a

balance between energy gain due to Coulomb interaction between the proton and the electron density in the bond and energy cost due to elastic energy required to move the Si atoms outward. Hypothetically, if the Si atoms initially were spaced further apart, the energy *gain* due to the formation of the three-center bond would still be the same, but the energy *cost* involved in moving the Si atoms would be lower, leading to a net increase in stability of the configuration. While this hypothesis is incompatible with the nature of pure *c*-Si, it is an attractive possibility in the case of poly-Si, where bond distortions near the grain boundaries are known to provide a variety of Si—Si bond distances.

This increase in stability of the BC configuration as a function of bond distortion was examined by Tarnow and Street (1992) and by Van de Walle and Nickel (1995); both studies employed first-principles pseudopotential-density-functional theory. Tarnow and Street (1992) investigated one aspect of the problem, namely, the effect of shear strain. Van de Walle and Nickel (1995) addressed bond-length variations as well as bond-angle variations.

Figure 12 summarizes the results for bond-stretching distortions (Van de Walle and Nickel, 1995). In this case, the Si atoms are displaced along the original bond direction. The circles in Fig. 12 indicate results for the change in formation energy expressed as a function of the *initial* distortion in the

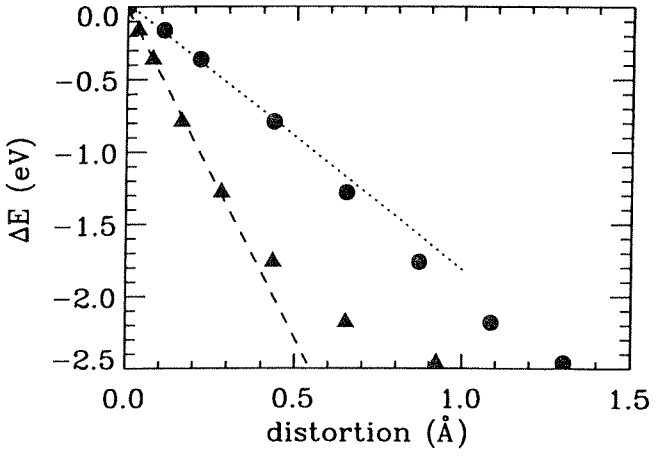


FIG. 12. Lowering in formation energy of the BC Si—H—Si configuration, for a bond-length distortion, as a function of *initial* distortion (circles) and as a function of the change in the *relaxed* bond length (triangles). For small distortions, the calculated points can be described by linear fits: 0.18 eV per 0.1 Å (dotted line) and 0.46 eV per 0.1 Å (dashed line).

Si—Si bond length. If relaxation is allowed, the Si atoms around the interface, of course, tend to move closer together, in order to try to restore the original Si—Si bond length. After relaxation, the change in bond length therefore will be smaller than given by the *initial* distortion; the triangles in Fig. 12 indicate results plotted as a function of the distortion in the *relaxed* bond length. For the configuration with H inserted in the bond, the Si atoms are, of course, also relaxed. The change in formation energy $\Delta E$ is always calculated using energy values for relaxed configurations, both in the absence and in the presence of hydrogen.

Figure 12 shows that for displacements up to 0.3 Å (which is the physical range of interest; see Sec. III.1), the behavior can be described adequately by a linear fit. Within the accuracy of the calculations, one finds a change in formation energy of 0.46 eV per 0.1 Å of increase in the (relaxed) Si—Si bond length. This value agrees quite well with a calculation by Li and Biswas (1995a, 1995b) for similar distortions in *a*-Si, as discussed in Section II.4. For bond-angle distortions, the results of Van de Walle and Nickel (1995) are in general agreement with the work of Tarnow and Street (1992). When the results were analyzed as a function of the increase in bond length that accompanies the bond-angle distortion, the behavior was found to be remarkably similar to that for pure bond-length distortions. The interesting conclusion was reached that for small displacements, no matter what the origin of the increase in bond length (be it pure bond stretching or bond bending), the formation energy of the Si—H—Si bond will be lowered by $\sim$0.4–0.5 eV per 0.1 Å of distortion in the Si—Si bond.

These results can now be combined with the information about bond-length distortions near grain boundaries that was discussed in Section III.1. The microscopic atomic structure near grain boundaries includes a significant number of bonds with bond lengths exceeding the bulk bond length. Changes in the bond length of 0.1 Å seem common; the theoretical results then indicate that the formation energy of H atoms inserted in such a stretched bond would be lowered by 0.4–0.5 eV; according to Fig. 11, this is precisely the amount needed to bring the formation energy in the range where it could explain the experimental observations of Nickel *et al.* (1994).

As discussed earlier, the Si—H—Si configuration has been identified as a donor in *c*-Si, with an energy level approximately 0.2 eV below the conduction band. Not surprisingly, this configuration continues to behave as a donor state if the Si—Si bonds are strained prior to inserting H. However, the donor level moves away from the conduction band as the bond becomes distorted, at a rate of $\sim$0.1 eV per 0.1 Å change in the bond length of the Si—Si bond (Van de Walle and Nickel, 1995). The experiments of Nickel *et al.* (1994) are not sensitive to the precise position of the donor level; indeed, the modification in the conductivity probably occurs through the introduc-

tion of charged defects at the grain boundary, which affect the depletion layers and hence the potential barriers at the boundaries (see Harbeke, 1985).

### 4. HYDROGEN-INDUCED GENERATION OF ACCEPTOR-LIKE DEFECTS

Prolonged exposure of poly-Si to monatomic hydrogen at elevated temperatures causes the generation of acceptor defects (Nickel *et al.*, 1995) (see also Sec. VI.1 of Chap. 4 in this volume). Type conversion was observed, and the acceptors were clearly established to be hydrogen induced. In contrast to the donor-type defects, for which a detailed microscopic model was discussed in the preceding subsection, the identification of the acceptor-type defects is more speculative at this stage. One explanation has been proposed, in terms of formation of hydrogen complexes with self-interstitial-type defects. These complexes, which were discussed in Section II.3, behave as acceptors, and it is plausible that their formation could be facilitated in the neighborhood of grain boundaries, which may have a tendency to form overcoordination defects (Kohyama and Yamamoto, 1994).

## IV. Conclusions and Future Directions

In this chapter I have attempted to review the current theoretical understanding of hydrogen interactions with amorphous and polycrystalline silicon, focusing on studies that build on computational approaches. Over the past decade, a wealth of information has been generated about the structural and energetic aspects of the interaction of hydrogen with *a*-Si. Some of this information was obtained from calculations on hydrogen interacting with *c*-Si; many interesting results can be produced in this fashion. Of course, explicit simulations of the amorphous networks are essential to provide information about energy distributions, H-H interactions and clustering, etc. Unfortunately, calculations for amorphous structures require large systems and are computationally very costly. Such calculations therefore are currently difficult to accomplish with first-principles techniques. Progress in this area can proceed along two paths: (1) improvements in algorithms (e.g., order-N methods) as well as computational efficiency and (2) development of computationally less demanding tight-binding or empirical-potential methods. Both approaches would allow calculations for increasingly larger and more realistic systems. They also

would allow molecular dynamics simulations on longer time scales.

While much progress has been made, I do not think we can claim to have a full understanding of the phenomenon of metastability in *a*-Si. It is my feeling that progress in this area will not come exclusively from being able to simulate increasingly larger systems. Advances also should focus on devising new experiments, accompanied by new theoretical analyses, for instance, on the effect of substituting hydrogen with deuterium.

For polycrystalline silicon, many challenges remain as well. Since most of the interesting features revolve around the grain boundaries, more accurate experimental and theoretical information about the structure of grain boundaries needs to be generated. This, in turn, will enable a microscopic picture of the interaction of hydrogen with the grain boundaries. In particular, the nature of the acceptor-like defects introduced during prolonged hydrogenation (Nickel *et al.*, 1995) requires further investigation.

## ACKNOWLEDGMENTS

Thanks are due to W. B. Jackson, J. Neugebauer, N. H. Nickel, and R. A. Street for productive collaborations, to R. Biswas, R. Jones, and B. Tuttle for constructive comments, and to N. Greenleaves for a critical reading of the manuscript.

## REFERENCES

Avouris, Ph., Walkup, R. E., Rossi, A. R., Shen, T.-C., Abeln, G. C., Tucker, J. R., and Lyding, J. W. (1996a). *Chem. Phys. Lett.*, **257**, 148.

Avouris, Ph., Walkup, R. E., Rossi, A. R., Akpati, H. C., Nordlander, P., Shen, T.-C., Abeln, G. C., and Lyding, J. W. (1996b). *Surface Science*, **363**, 368.

Bar-Yam, Y., and Joannopoulos, J. D. (1984). *Phys. Rev. Lett.*, **52**, 1129.

Bech Nielsen, B. (1991). *Phys. Rev. Lett.*, **66**, 2360.

Bech Nielsen, B., Hoffmann, L., Budde, M., Jones, R., Goss, J., and Öberg, S. (1995). *Mater. Sci. Forum*, **196–201**, 933.

Bigger, J. R. K., McInnes, D. A., Sutton, A. P., Payne, M. C., Stich, I., King-Smith, R. D., Burd, D. M., and Clarke, L. J. (1992). *Phys. Rev. Lett.*, **69**, 2224.

Biswas, R., Kwon, I., and Soukoulis, C. M. (1991). *Phys. Rev. B*, **44**, 3403.

Blöchl, P. E., Smargiassi, E., Car, R., Laks, D. B., Andreoni, W., and Pantelides, S. T. (1993). *Phys. Rev. Lett.*, **70**, 2435.

Bourret, A. (1985). In *Polycrystalline Semiconductors: Physical Properties and Applications*, **57**, G. Harbeke, ed. Berlin: Springer, p. 2.

Branz, H. M., Asher, S., Nelson, B. P., and Kemp, M. (1993). *J. Non-Cryst. Solids*, **164–166**, 269.

Buda, F., Chiarotti, G. L., Car, R., and Parrinello, M. (1991). *Phys. Rev. B*, **44**, 5908.

Buda, F., Chiarotti, G. L., Stich, I., Car, R., and Parrinello, M. (1992). *J. Non-Cryst. Solids*, **114**, 7.
Car, R., and Parrinello, M. (1985). *Phys. Rev. Lett.*, **55**, 2471.
Car, R., Kelly, P. J., Oshiyama, A., and Pantelides, S. T. (1985). *Phys. Rev. Lett.*, **54**, 360.
Carlson, D. E., and Magee, C. W. (1978). *Appl. Phys. Lett.*, **33**, 81.
Chang, K. J., and Chadi, D. J. (1989). *Phys. Rev. Lett.*, **62**, 937.
Cohen, J. D., Leen, T. M., and Rasmussen, R. J. (1992). *Phys. Rev. Lett.*, **69**, 3358.
Cowern, N. E. B., van de Walle, G. F. A., Zalm, P. C., and Vandenhoudt, D. W. E. (1994). *Appl. Phys. Lett.*, **65**, 2981.
Dabrowski, J., Müssig, H.-J., and Wolff, G. (1994). *Phys. Rev. Lett.*, **73**, 1660.
DiVincenzo, D. P., Bernholc, J., and Brodsky, M. H. (1983). *Phys. Rev. B*, **28**, 3246.
DiVincenzo, D. P., Alerhand, O. L., Schlüter, M., and Wilkins, J. W. (1986). *Phys. Rev. Lett.*, **56**, 1925.
Drabold, D. A., Fedders, P. A., Sankey, O. F., and Dow, J. D. (1990). *Phys. Rev. B*, **42**, 5135.
Eaglesham, D. J., Stolk, P. A., Gossmann, H.-J., and Poate, J. M. (1994). *Appl. Phys. Lett.*, **65**, 2305.
Estreicher, S. K. (1995). *Mater. Sci. Engr. Reps.*, **14**, 319.
Fedders, P. A. (1995). *Phys. Rev. B*, **52**, 1729.
Fedders, P. A., and Drabold, D. A. (1993). *Phys. Rev. B*, **47**, 13277.
Fedders, P. A., and Drabold, D. A. (1996). *Phys. Rev. B*, **53**, 3841.
Fisch, R., and Licciardello, D. C. (1978). *Phys. Rev. Lett.*, **41**, 889.
Guttman, L. (1981). *Phys. Rev. B*, **23**, 1866.
Guttman, L., and Fong, C. Y. (1982). *Phys. Rev. B*, **26**, 6756.
Guyot-Sionnest, P., Dumas, P., Chabal, Y. J., and Higashi, G. S. (1990). *Phys. Rev. Lett.*, **64**, 2156.
Guyot-Sionnest, P., Lin, P. H., and Miller, E. M. (1995). *J. Chem. Phys.*, **102**, 4269.
Hamann, D. R., Schlüter, M., and Chiang, C. (1979). *Phys. Rev. Lett.*, **43**, 1494.
Harbeke, G., ed. (1985). *Polycrystalline Semiconductors: Physical Properties and Applications*, Springer Series in Solid-State Sciences, **57**, part II, M. Cardona, ed. Berlin: Springer-Verlag.
Harris, J. (1985). *Phys. Rev. B*, **31**, 1770.
Herring, C., and Johnson, N. M. (1991). In *Semiconductors and Semimetals*, **34**, J. I. Pankove and N. M. Johnson, eds. San Diego: Academic Press, p. 279.
Hohenberg, P., and Kohn, W. (1964). *Phys. Rev.*, **136**, B864.
Jackson, W. B. (1990). *Phys. Rev. B*, **41**, 10257.
Jackson, W. B., and Kakalios, J. (1989). In *Advances in Disordered Semiconductors*, **1A**, H. Fritzsche, ed. Singapore: World Scientific, p. 247.
Jackson, W. B., and Tsai, C. C. (1992). *Phys. Rev. B*, **45**, 6564.
Jackson, W. B., Johnson, N. M., and Biegelsen, D. K. (1983). *Appl. Phys. Lett.*, **43**, 882.
Johnson, N. M., Biegelsen, D. K., and Moyer, M. D. (1982). *Phys. Rev. Lett.*, **40**, 882.
Johnson, N. M., Ponce, F. A., Street, R. A., and Nemanich, R. J. (1987). *Phys. Rev. B*, **35**, 4166.
Johnson, N. M., Herring, C., Doland, C., Walker, J., Anderson, G., and Ponce, F. (1991). In *Proceedings of the 16th International Conference on Defects in Semiconductors*, G. Davies, G. G. DeLeo, and M. Stavola, eds. Zürich: Trans Tech, p. 33.
Johnson, N. M., Herring, C., and Van de Walle, C. G. (1994). *Phys. Rev. Lett.*, **73**, 130.
Jones, R. (1991). *Physica B*, **170**, 181.
Jones, R. (1997). Private communication.
Jones, R., and Lister, G. M. S. (1990). *Philos. Mag. B*, **61**, 881.
Kakalios, J., Street, R. A., and Jackson, W. B. (1987). *Phys. Rev. Lett.*, **59**, 1037.
Keblinski, P., Philpot, S. R., Wolf, D., and Gleiter, H. (1997). *J. Am. Cer. Soc.*, **80**, 717.

Kemp, M., and Branz, H. M. (1993). *Phys. Rev. B*, **47**, 7067.
Kemp, M., and Branz, H. M. (1995). *Phys. Rev. B*, **52**, 13946.
Kohn, W., and Sham, L. J. (1965). *Phys. Rev.*, **140**, A1133.
Kohyama, M., and Takeda, S. (1992). *Phys. Rev. B*, **46**, 12305.
Kohyama, M., and Yamamoto, R. (1994). *Phys. Rev. B*, **50**, 8502.
Lee, I.-H., and Chang, K. J. (1994). *Phys. Rev. B*, **50**, 18083.
Li, Q., and Biswas, R. (1994a). *Phys. Rev. B*, **50**, 18090.
Li, Q., and Biswas, R. (1994b). *Mater. Res. Soc. Symp. Proc.*, **336**, 219.
Li, Q., and Biswas, R. (1995a). *Phys. Rev. B*, **52**, 10705.
Li, Q., and Biswas, R. (1995b). *Mater. Res. Soc. Symp. Proc.*, **377**, 407.
Li, Q., and Biswas, R. (1996). *Appl. Phys. Lett.*, **68**, 2261.
Lyding, J. W., Shen, T. C., Hubacek, J. S., Tucker, J. R., and Abeln, G. C. (1994). *Appl. Phys. Lett.*, **64**, 2010.
Lyding, J. W., Hess, K., and Kizilyalli, I. C. (1996). *Appl. Phys. Lett.*, **68**, 2526.
Madelung, O., ed. (1991). *Data in Science and Technology: Semiconductors.* Berlin: Springer-Verlag.
Nelson, J. S., Fong, C. Y., Guttman, L., and Batra, I. (1988). *Phys. Rev. B*, **37**, 2622.
Nickel, N. H., Johnson, N. M., and Jackson, W. B. (1993a). *Appl. Phys. Lett.*, **62**, 3285.
Nickel, N. H., Jackson, W. B., and Johnson, N. M. (1993b). *Phys. Rev. Lett.*, **71**, 2733.
Nickel, N. H., Johnson, N. M., and Van de Walle, C. G. (1994). *Phys. Rev. Lett.*, **72**, 3393.
Nickel, N. H., Johnson, N. M., and Walker, J. (1995). *Phys. Rev. Lett.*, **75**, 3720.
Nickel, N. H., Anderson, G. B., and Walker, J. (1996). *Solid State Commun.*, **99**, 427.
Northrup, J. E. (1989). *Phys. Rev. B*, **40**, 5875.
Pankove, J. I., and Johnson, N. M., eds. (1991). *Hydrogen in Semiconductors, Semiconductors and Semimetals*, **34**. San Diego: Academic Press.
Pantelides, S. T. (1986). *Phys. Rev. Lett.*, **57**, 2979.
Pantelides, S. T. (1987a). *Phys. Rev. Lett.*, **58**, 1344.
Pantelides, S. T. (1987b). *Phys. Rev. B*, **36**, 3479.
Pearton, S. J., Corbett, J. W., and Stavola, M. (1992). *Hydrogen in Crystalline Semiconductors.* Berlin: Springer-Verlag.
Ponce, F. A., Johnson, N. M., Tramontana, J. C., and Walker, J. (1987). In *Proceedings of the Microscopy of Semiconductivity Materials Conference*, A. G. Cullis, ed. *Inst. Phys. Conf. Ser.* **87**. London: Adam Hilger, Ltd., p. 49.
Queisser, H. J. (1983). *Mater. Res. Soc. Symp. Proc.*, **14**, 323.
Sankey, O. F., and Niklewski, D. J. (1989). *Phys. Rev. B*, **40**, 3979.
Sankey, O. F., and Drabold, D. A. (1991). *Bull. Am. Phys. Soc.*, **36**, 924.
Santos, P. V., and Jackson, W. B. (1992). *Phys. Rev. B*, **46**, 4595.
Santos, P., and Johnson, N. M. (1993). *Appl. Phys. Lett.*, **62**, 720.
Santos, P., Johnson, N. M., and Street, R. A. (1991). *Phys. Rev. Lett.*, **67**, 2686.
Shen, T.-C., Wang, C., Abeln, G. C., Tucker, J. R., Lyding, J. W., Avouris, Ph., and Walkup, R. E. (1995). *Science*, **268**, 1590.
Smith, Z. E., and Wagner, S. (1987). *Phys. Rev. Lett.*, **59**, 688.
Staebler, D. L., and Wronski, C. R. (1977). *Appl. Phys. Lett.*, **31**, 292.
Street, R. A. (1987). *Mater. Res. Symp. Proc.*, **95**, 13.
Street, R. (1991a). In *Hydrogenated Amorphous Silicon.* Cambridge: Cambridge University Press.
Street, R. (1991b). *Physica B*, **170**, 69.
Street, R. (1991c). *Phys. Rev. B*, **43**, 2454.
Street, R. A., and Winer, K. (1989). *Phys. Rev. B*, **40**, 6236.
Street, R., Tsai, C. C., Kakalios, J., and Jackson, W. B. (1987). *Philos. Mag. B*, **56**, 305.

Stutzmann, M., Jackson, W. B., and Tsai, C. C. (1985). *Phys. Rev. B*, **32**, 23.
Tan, T. Y. (1981). *Philos. Mag. A*, **44**, 101.
Tarnow, E., and Street, R. A. (1992). *Phys. Rev. B*, **45**, 3366.
Tarnow, E., Bristowe, P. D., Joannopoulos, J. D., and Payne, M. C. (1989). In *Atomic Scale Calculations in Materials Science*, J. Tersoff, D. Vanderbilt, and V. Vitek, eds. Materials Research Society Symposia Proceedings, Vol. 141. Pittsburgh: Materials Research Society, p. 333.
Tarnow, E., Dallot, P., Bristowe, P. D., Joannopoulos, J. D., Francis, G. P., and Payne, M. C. (1990). *Phys. Rev. B*, **42**, 3644.
Thomson, R. E., and Chadi, D. J. (1984). *Phys. Rev. B*, **29**, 889.
Tuttle, B., and Adams, J. (1996). *Phys. Rev. B*, **53**, 16265.
Tuttle, B., and Adams, J. (1997). *Phys. Rev. B*, **56**, 4565.
Tuttle, B., and Adams, J. (1998). *Phys. Rev. B*, **57**, 12859.
Tuttle, B., and Van de Walle, C. G. (1999). *Phys. Rev. B*, in press.
Tuttle, B., Van de Walle, G. G., and Adams, J. (1999). *Phys. Rev. B*, in press.
Van de Walle, C. G. (1991a). In *Hydrogen in Semiconductors*, **34**, J. I. Pankove and N. M. Johnson, eds. San Diego: Academic Press, p. 585.
Van de Walle, C. G. (1991b). *Physica B*, **170**, 21.
Van de Walle, C. G. (1994). *Phys. Rev. B*, **49**, 4579.
Van de Walle, C. G. (1996a). *Phys. Rev. B*, **53**, 11292.
Van de Walle, C. G. (1996b). In *Amorphous Silicon Technology*, M. Hack, R. Schropp, E. A. Schiff, A. Matsuda, and S. Wagner, eds. Pittsburgh: Materials Research Society, p. 533.
Van de Walle, C. G., and Street, R. A. (1994). *Phys. Rev. B*, **49**, 14766.
Van de Walle, C. G., and Street, R. A. (1995). *Phys. Rev. B*, **51**, 10615.
Van de Walle, C. G., and Nickel, N. H. (1995). *Phys. Rev. B*, **51**, 2636.
Van de Walle, C. G., and Neugebauer, J. (1995). *Phys. Rev. B*, **52**, R14320.
Van de Walle, C. G., and Jackson, W. B. (1996). *Appl. Phys. Lett.*, **69**, 2441.
Van de Walle, C. G., Denteneer, P. J. H., Bar-Yam, Y., and Pantelides, S. T. (1989). *Phys. Rev. B*, **39**, 10791.
Van Wieringen, A., and Warmoltz, N. (1956). *Physica*, **22**, 849.
Walsh, R. (1981). *Acc. Chem. Res.*, **14**, 246.
Watkins, G. D. (1991). In *Materials Science and Technology*, **4**, Cahn, Haasen, and Kramer, eds. Weinheim: VCH, p. 107.
Zacher, R., Allen, L. C., and Licciardello, D. C. (1986). *J. Non-Cryst. Solids*, **85**, 13.
Zhang, S. B., and Jackson, W. B. (1991). *Phys. Rev. B*, **43**, 12142.
Zhang, S. B., Jackson, W. B., and Chadi, D. J. (1990). *Phys. Rev. Lett.*, **65**, 2575.